Naval Research Reviews

Office of Naval Research
Two/1994
Vol XLVI

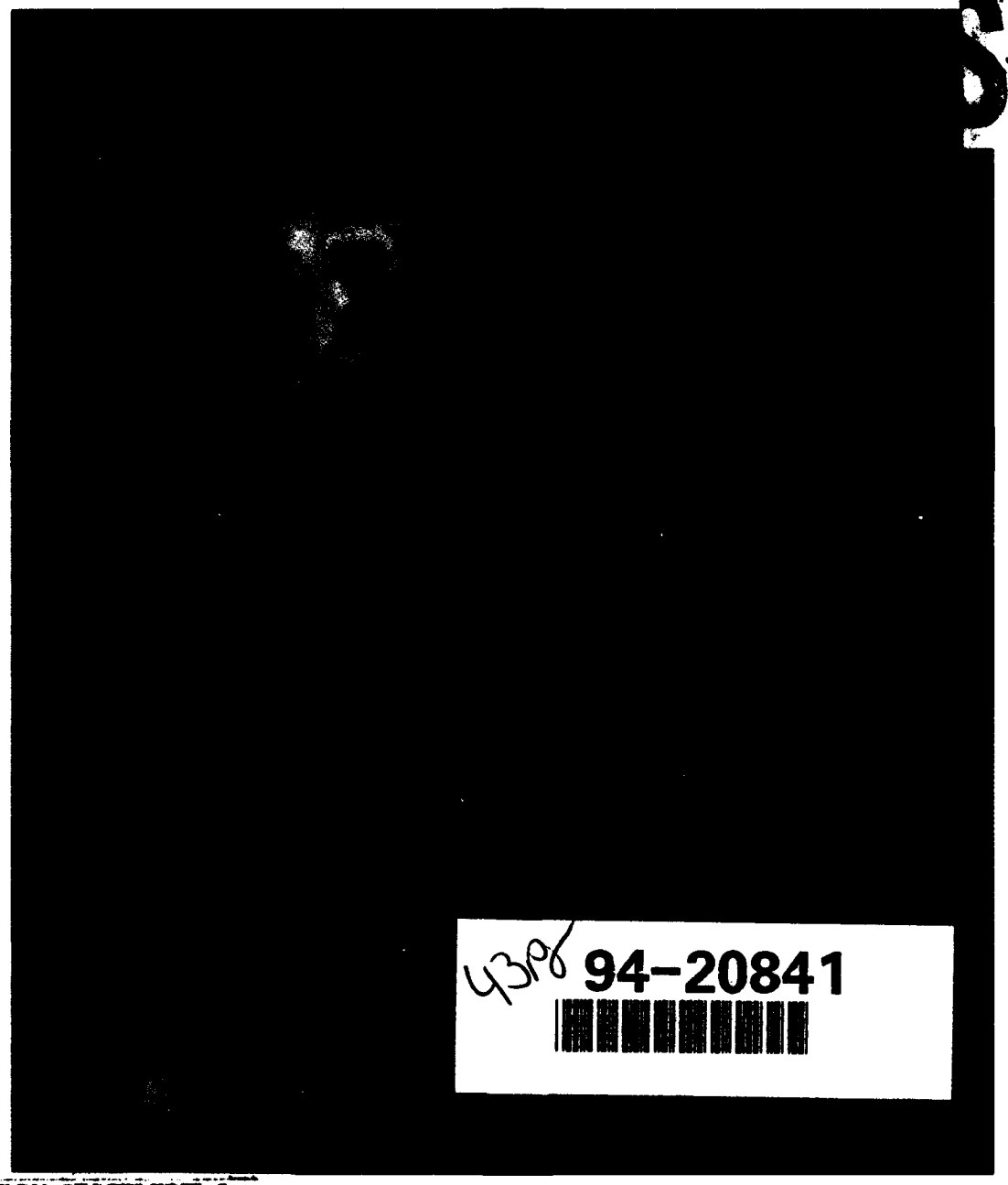

Isabella Karle

Winner of the 1993 Bower Award in Science

Isabella Karle Honored

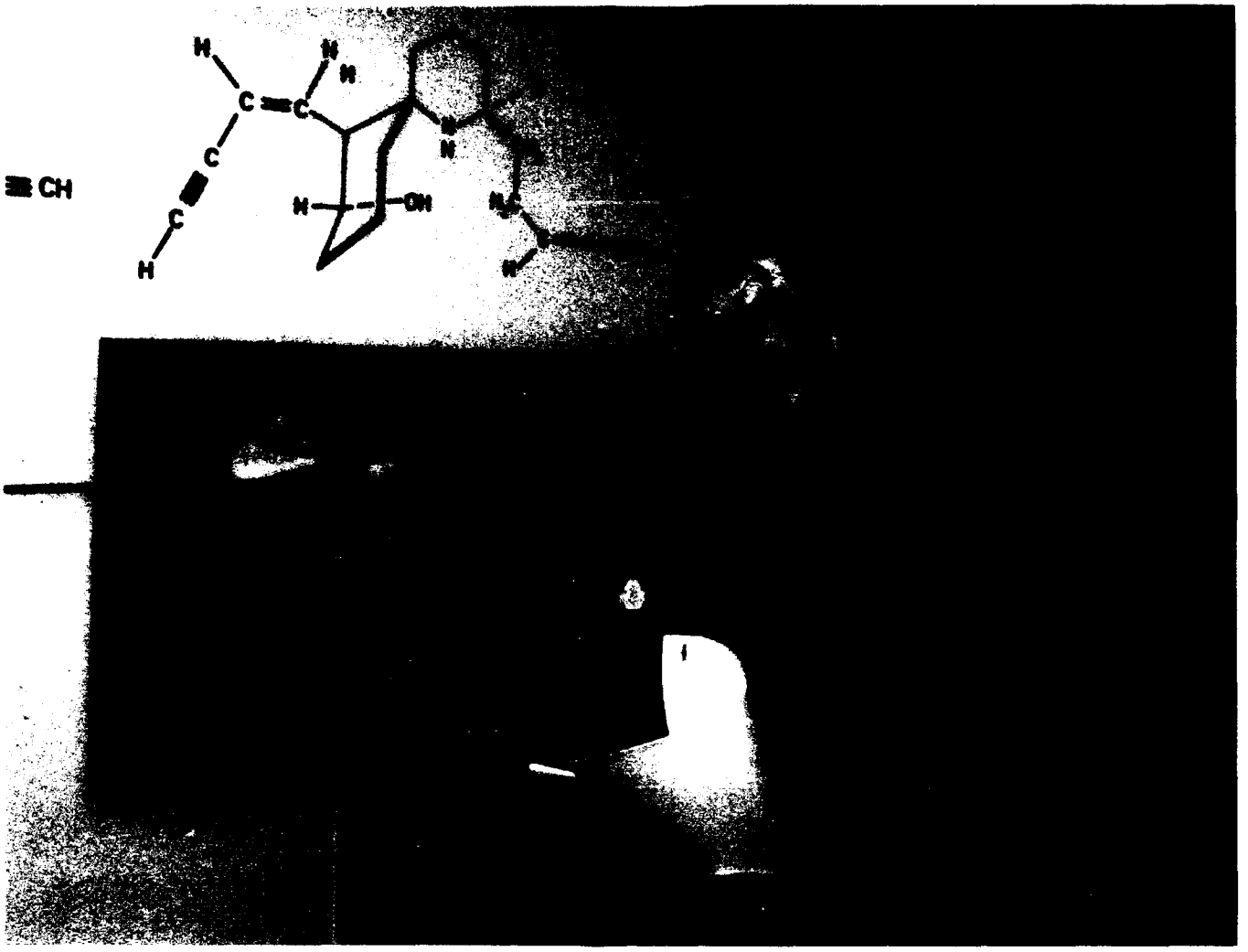

The Franklin Institute announced on November 17 at a ceremony in Washington that Dr. Isabella Lugoski Karle is the 1993 recipient of the Bower Award for Science, which consists of a gold medal and $250,000. Dr. Karle is the first women to receive the prestigious annual award of the Franklin Institute which was founded in 1834 to promote scientific inquiry and achievement. The award will be presented April 7, 1994.

Dr. Karle, who is a senior scientist specializing in crystallography at the Naval Research Laboratory, is honored for her pioneering work in developing electron and X-ray diffraction techniques that make immediate determination of the three-dimensional structure of molecules possible. Her inventive work bridged the gap between the theoretical formulas for crystal structure determination and the practical methodology required to achieve useful applications. This has facilitated research in chemistry, biology, and medicine. Dr. Karle's own studies have included crystallographic analyses of photorearrangement products, ionophores, peptides, toxins, antitoxins, cardioactive substances and natural analgesics.

A native of Detroit, Michigan, Dr. Karle won a scholarship to the University of Michigan where she earned B.S., M.S. and Ph.D degrees with a specialty in physical chemistry. While at Michigan, she married Dr. Jerome Karle; and they both came to NRL in 1946. Dr. Jerome Karle is Chief Scientist of the Laboratory for the Structure of Matter at NRL. His work in crystal structure analysis was recognized by the 1985 Nobel Prize in Chemistry. Dr. Isabella Karle often collaborates with her husband on research projects.

Naval Research Reviews

Office of Naval Research
Two/1994
Vol XLVI

Articles

Departments

About the Cover

Dr. Isabella Karle, a Senior Scientist of the Naval Research Laboratory, at the ceremony honoring her selection for the 1993 Bower Award in Science by the Franklin Institute of Philadelphia. A renowned physical chemist and crystallographer, she is recognized for determining the three dimentional structure of molecules making use of both X-ray and electron diffraction.

Naval Research Reviews publishes articles about research conducted by the laboratories and contractors of the Office of Naval Research and describes important naval experimental activities. Manuscripts submitted for publication, correspondence concerning prospective articles, and changes of address, should be directed to Code OPARI, Office of Naval Research, Arlington, VA 22217-5000. Requests for subscriptions should be directed to the Superintendent of Documents, U.S. Government Printing Office, Washington, DC 20403. *Naval Research Reviews* is published from appropriated funds by authority of the Office of Naval Research in accordance with Navy Publications and Printing Regulations. NAVSO P-35.

Remarks At The Bower Award Reception For Isabella Karle Navy Museum, Washington Navy Yard November 18, 1993

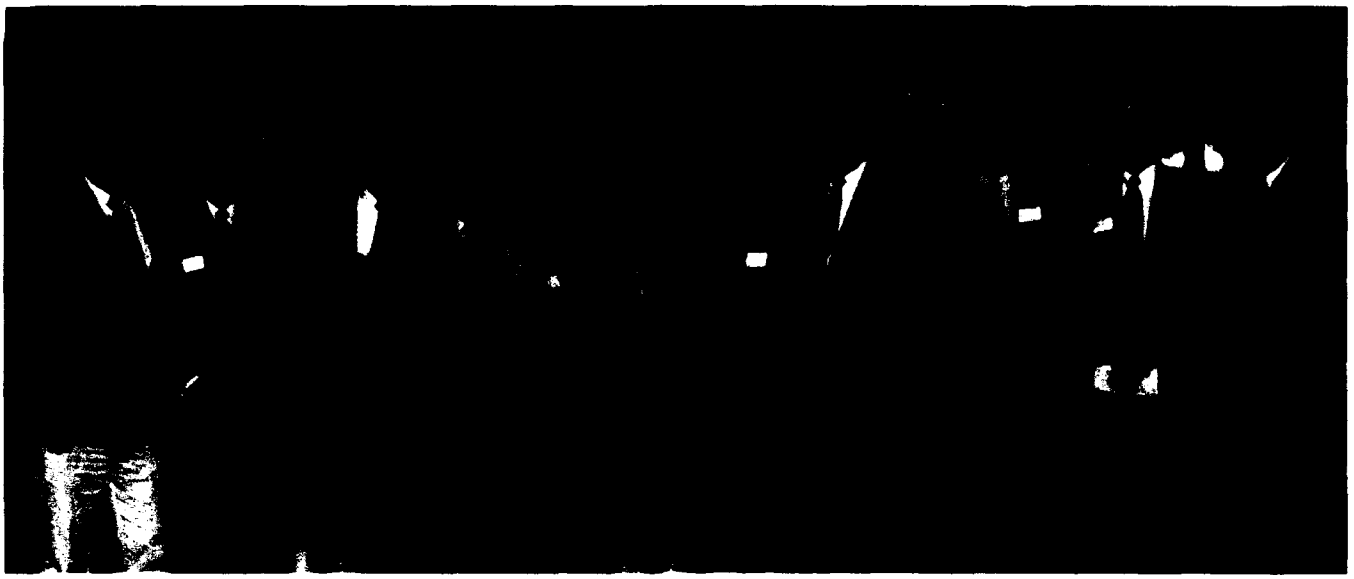

Left to right: Dr. Fred Saalfeld, Deputy Chief of Naval Research; RADM Marc Pelaez, Chief of Naval Research; the Honorable Nora Slatkin, Assistant Secretary of Navy (Research, Development and Acquisition); Dr. Timothy Coffey, NRL Director of Research; Madeleine Tawney; Dr. Jerome Karle; Dr. Jean Karle; Dr. Isabella Karle: the Honorable Anita K. Jones, Director, Defense Research and Engineering; the Honorable John H. Dalton, Secretary of the Navy; Dr. Larry Tise, Executive Director, Franklin Memorial; Dr. James L. Powell, President, Franklin Institute; and CAPT Paul G. Gaffney II, NRL, Commanding Officer.

CAPT Gaffney: The nation's Naval Research Laboratory (NRL) is honored to assist the historic and renowned Franklin Institute and Franklin Memorial, this evening, in its formal announcement of the prestigious Bower Award and Prize for Scientific Achievement.

We have a very short program featuring several top leaders in national science and defense policy. So, without further ado, it is my distinct pleasure to introduce to you, President and Chief Executive Officer of the Franklin Institute, Dr. James L. Powell, and Dr. Larry Tise, the Executive Director of the Franklin Memorial.

Dr. Powell: Thank you very much Captain Gaffney. Good evening everyone.

It was a former Assistant Secretary of the Navy, Franklin Delano Roosevelt, who said "When you're giving a talk after dinner be sincere, be brief, be seated." So, I'm going to try to follow his advice this evening, but it's a great honor for me personally to be here as a scientist. I've known about the important work of NRL and its various incarnations all my career and I'm very privileged to be here.

The Franklin Institute was founded in 1824 to promote the "mechanic arts," as they referred to them in those days, and we've been doing science, in one way or another, ever since. One of the things that those of us who are concerned about science realize is that we do not have a very favorable image. The media does not help. Instead of encouraging children to go into science, they seem to have just the opposite effect, and so I think we need to seize every opportunity that we have to recognize scientific achievement.

I was very pleased when I got to the Franklin Institute a few years ago to find out that we have a distinguished program for recognizing scientific achievement. And, when that achievement goes to a woman or a member of a minority group, so much the better, because those are the people we especially need to encourage into science. In just a moment, Dr. Tise, my colleague, will say a bit about the process by which the awardee is selected, and you will see that it is a result of an international search whose ground rules are only that we try to find the very best person that we can in science. Just to show you the conclusion that we came to about Dr.

Karle, before I turn to Dr. Tise, I want to read you part of the citation that will be presented to her and is the basis for this award. "The Bower Award and Prize in Science goes to Isabella L.Karle, physical chemist and crystallographer, for pioneering contributions in determining the three dimensional structure of molecules, making use of both X-ray and electron diffraction, and, in particular, for her definitive introduction of a procedure to reveal molecular structure directly from X-ray studies. This inventive work has profoundly facilitated studies in chemistry, biology, and medicine, permitting routine and immediate determinations of molecular structures. She has thrived in her profession and served as an inspiration to her colleagues and students with a curiosity and creativity that make her a kindred spirit of Benjamin Franklin himself." So, we are very pleased to be able to make this award to Dr. Karle. And now, I'd like to turn to Larry Tise.

The Honorable John H. Dalton, Secretary of the Navy.

Dr. Tise: Not as a scientist but an historian, I was very pleased, when I came to the Franklin Institute some five years ago, and had the responsibility of establishing the procedures for the Bower Award, to find that my chief mission was to find that individual in our world today, every year, who reflects the scientific and humanitarian genius of Benjamin Franklin.

In setting up the process of finding this person every year, we established a worldwide nomination process, an international board of advisors; we established a selection process that is more rigorous, or equally rigorous, to any other award in the world and, every year, we receive thousands of inquiries about this award. After discouraging many people from submitting a nomination, we receive between 50 and 100 fully documented nominations, which are then reviewed on three levels; locally, among scientists in our community and then internationally, among scientists who are expert in the field of the nomination, and then, finally, we bring together an international selection committee of people, mainly not from the United States, to help us decide who should receive the award in this particular year.

This year Isabella Karle was selected not only because of an outstanding scientific achievement that you just heard Dr. Powell describe, but also because her work has applications in so many fields. I wish you could have heard the selection committee when they discussed this nomination and made the selection. They said, "Karle and Karle." It is known to everybody all over the world and because of her life and contributions, not only as a scientist, but also as a citizen and, particularly in this year, as an inspiration to women to choose careers in science. It has been my pleasure to sort of guide and direct this process this year and to come to know Dr. Karle.

I would like to invite all of you to Philadelphia on April 7th and 8th, next year, when we will not only present her with a check and with a gold medal, but we will be holding two days, actually three days, of events in which we will be exploring the work that she has done and that others in her field have done, and we will be looking at related issues, such as the role of women in science today. We will celebrate her work and, of course, we'll spend some time talking about Benjamin Franklin as well. Thank you.

CAPT Gaffney: Ladies and gentlemen, in his first appearance in connection with science and technology, the Honorable John H. Dalton, Secretary of the Navy.

Secretary Dalton: Thank you very much, and I want to welcome each of you here tonight to this beautiful museum. Several people, during the cocktail hour, mentioned to me that this is the first time they had been in this building and I hope that you'll come back and take it in. It really is a wonderful place and we're fortunate to have it.

I'm very pleased to be here tonight on this occasion. It's a tremendous day for the Department of the Navy and it's great that we're here to honor Dr. Isabella Karle, as the

recipient of the 1993 Bower Award and Prize for Achievement in Science. The Bower Award, which recognizes outstanding achievement in the life or physical sciences, serves as a memorial to that great American scientist and humanitarian, diplomat and patriot, Benjamin Franklin. Dr. Karle's scientific achievements stand solemnly within the tradition established by Benjamin Franklin. A tradition that combines scientific excellence with public service. The great Franklin once advised a friend to continue with his "excellent experiments...produce facts, improve science and do good to mankind." Dr. Isabella Karle has excelled in all these regards. An outstanding researcher, laboratory teacher, lifelong civil servant and parent, she has set an example to which her colleagues and succeeding generations of scientists can aspire. She has indeed carried out excellent experiments, produced facts, improved science, and done good to mankind. At the same time, she has raised a family of achievers in their own right.

As Secretary of the Navy, I'm especially pleased that the Department of the Navy can claim Isabella as its own. Her work stands as an example for the high quality research carried out by the men and women at the Naval Research Laboratory. We, in the Navy, are fortunate to have developed and maintained a national resource like NRL, which can attract and retain world class scientists, like Isabella and her husband, Nobel Laureate, Dr. Jerome Karle. Dr. Isabella Karle's career spans over 47 years with the Navy, at the Naval Research Laboratory. After receiving her Ph.D. in chemistry, at the age of 22, she and her husband both worked on the Manhattan project. Both were subsequently appointed to NRL. Isabella's efforts for our Navy and our nation have combined hard work with insights into the processes of nature. Dr. Karle's master work is her now famous symbolic addition procedure for determining molecular structures, an advance that has greatly aided medical and pharmaceutical research. The author of almost 300 scientific papers and the recipient of numerous awards and citations, including the Secretary of the Navy's Distinguished Achievement Award in Science, Dr. Isabella Karle is the only woman ever elected to the Chemistry Section of the National Academy of Sciences and now she is the first woman and first US government scientist to win the Bower Award and Prize. As the Department of the Navy right-sizes and reshapes its forces with a post-cold-war world, science and technology become evermore important in continuously improving our capabilities to use the sea and preserve peace.

Great institutions such as the Naval Research Laboratory and the Franklin Institute as well as dedicated scientists like Dr. Karle are critical if we are to be successful in these efforts. They will provide the foundation for America's future.

On behalf of the President of the United States and the Department of the Navy, I am very proud to be here to personally congratulate Dr. Isabella Karle on her selection to receive the Franklin Institute's Bower Award and Prize for Achievement in Science. Isabella, we're proud of you. Congratulations and God bless you.

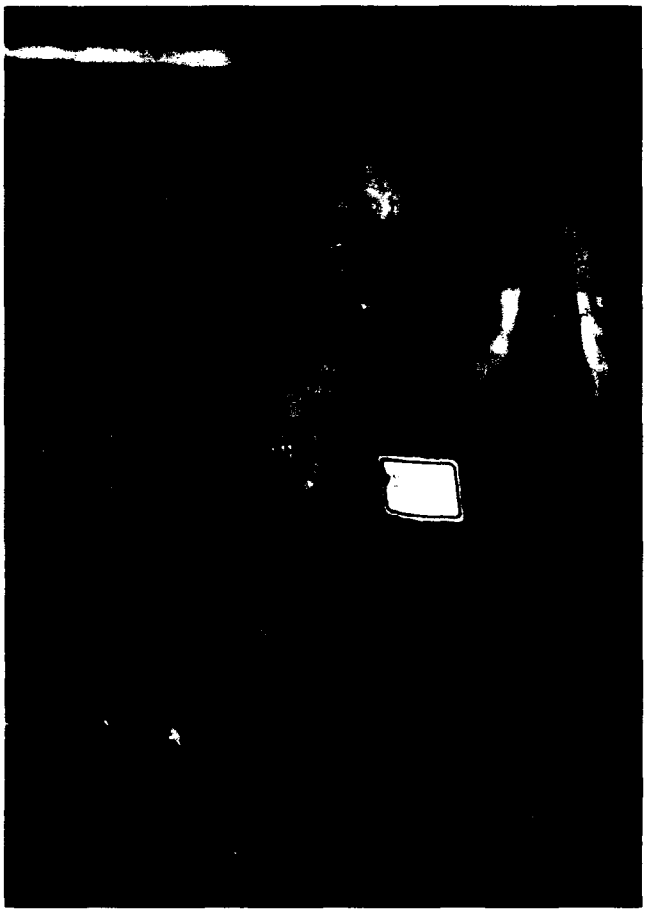

The Honorable Anita K. Jones, Director, Defense Research and Engineering.

CAPT Gaffney: Thank you Mr. Secretary. Ladies and gentlemen, the champion of defense science and technology, and I'm very pleased to say a rather frequent visitor to the Naval Research Laboratory. It's my pleasure to introduce the Director of Defense Research and Engineering (DDR&E), the Honorable Anita K. Jones.

Dr. Jones: Thank you Capt. Gaffney, and Secretary Dalton, Dr. Powell and Dr. Karle.

It's an honor to join with this group of guests to celebrate the announcement of the award of the Bower Prize to Dr. Isabella Karle. It's a particular pleasure to recognize this prize going to a renowned scientist from within the Department of Defense community.

My first speech when I became the DDR&E was at the Naval Research Laboratory. It was at a seminar on contemporary science honoring Dr. Jerry Karle on the occasion of his 75th birthday, and now I have the pleasure of being here. When I walked in, I had intended to ask whether there are some other members of the family that I should be on the lookout for. I was sitting next to Dr. Karle and she pointed

Dr. Isabella Karle, Naval Research Laboratory Senior Scientist and recipient of the 1993 Bower Award.

out that the radiation-related material depicted in the left-hand panel of the display over here was the result of collaboration with a daughter. So I did not need to ask.

An award like this, among other things, recognizes quality, and quality is crucial in a scientific enterprise. It's particularly my job, and a fine one I may add, to try to defend, to catalyze, and to find new opportunities for injecting quality into the science and technology program of the Department of Defense. Also it's a real pleasure to see work of the highest distinction recognized by an award as eminent as the Bower Award from the Franklin Institute. Such an award spills over to the colleagues and to the environment in which a scientist works. I think the Naval Research Laboratory can be very proud of its support and the conditions it made possible, and which played a part in this award as well.

It's very difficult to express to someone who's not a scientist how exciting it can be and what a difference a single individual can make. Also it is difficult to make a description of Dr. Karle in down-home terms - I'm from Texas. One of the things she is noted for is creating electron and X-ray diffraction techniques, that allow one to see 3-D structures that you couldn't see before and, so, a way of describing her work is: "she gave eyes to scientists across the world to see what they could not see before her." To see into what was darkness before – that is a very exciting experience. Dr. Karle is the first woman, as Secretary Dalton said, to receive this Franklin Institute Award and it's a particular pleasure for me to join this company, in recognizing her, and to know that we have such high recognition of a woman who is a role model for both men and women, but particularly women, who are moving through the defense laboratory science community.

It is a pleasure to offer my congratulations to you Dr. Karle. I'd like to close by bringing to you a message from Les Aspin, the Secretary of Defense. He writes,

"It is my pleasure to congratulate Dr. Isabella Karle for winning the 1993 Franklin Institute Bower Award and Prize for Achievement in Science. This award is a testament to Dr. Karle's outstanding career as a physical chemist and crystallographer. Her work at the Naval Research Laboratory has enormous implications for the advancement of chemistry, biology, and medicine. Not only is Dr. Karle the first woman to win the highly prestigious Bower Science Award, she is also the first recipient from the community of Defense Department laboratories. We're very proud of her. Defense research has been very successful in making our armed forces the world's best. Dr. Karle's recognition also underscores the potential for private sector uses of the technologies developed in our military laboratories.

"In honoring Dr. Karle and her work, the Franklin Institute is highlighting the benefits of technology transfer from the military to the civilian sector. We are deeply grateful for that recognition by the institute. This ceremony provides a wonderful means of expressing gratitude to Dr. Karle. I appreciate the opportunity to add my thanks for her many remarkable contributions to science and to our nation."

CAPT Gaffney: Ladies and gentleman, reflecting on her magnificent career, addressing Navy and national scientific challenges, the senior scientist in NRL's Laboratory for the Structure of Matter is the 1993 Bower Award selectee, Dr. Isabella Karle.

Dr. Karle: Thank you Dr. Powell, Secretary Dalton, Dr. Tise, Secretary Jones for this magnificent event. I am indeed honored, excited, and grateful to have been named the recipient of the Bower Award. I wish to thank the trustees of the Franklin Institute and the selection committee for all their hard work. I also deeply appreciate having been nominated by Dr. Coffey, the Director of Research, the Naval Research Laboratory and Dr. Rath, the Associate Director for Material Science.

The Naval Research Laboratory deserves much credit for supporting basic research and for providing a suitable and

The Honorable Nora Slatkin, Assistant Secretary of the Navy (Research, Development and Acquisition) to the left and Dr. Isabella Karle.

exciting environment for science to flourish. When my husband and I first arrived at the Laboratory 47 years ago, we were immediately thrust into an atmosphere of exciting research and surrounded by exceptional people, whose names still appear on the front page of the Laboratory newspaper and one of whom is here at this gathering. Dr. Herbert Friedman was our immediate supervisor and, as most of you know, he has won world acclaim for spatial astronomy and was presented with very many awards, amongst them the Wolf Prize of Israel of 1987. Dr. Richard Tousey was just a few doors down the hall and he, in 1990, received the Hale Prize for solar spectroscopy. Somewhat later, Dr. Timothy Coffey and Dr. Bhakta Rath, of course, they're younger so they had to be later, came to the Laboratory and they too have prestigious awards. Dr. Coffey received the 1991 Franklin Institute Delmer Fahrney Medal for leadership in science and technology. Dr. Bhakta Rath received the 1992 Minerals, Medals, and Materials Society Award for Materials Science. Almost anytime we open *Labstracts*, which is the Laboratory newspaper, there is someone who is receiving an important award. Last week, I think it was, Dr. Robert Lehmberg and Dr. Richard Obenschain received the American Physical Society Award for Excellence in Plasma Physics. So, you see, these are only a very few examples of the national and international recognition accorded to NRL scientists, and that makes NRL an important and interesting place to work, especially since all of these people received their awards in rather diverse fields of science. The mood, prevalent in the Laboratory when we first came in the late 1940s, can be measured by the following occurrence. Jerome designed an electron diffraction apparatus, which was very large and complicated and I assembled the pieces, aligned and fine-tuned all the components, and eventually collected and analyzed data. Well, during the process of building the apparatus, when the on-site foundry and machine shops were supposed to cast and fabricate the large brass segments, Captain Brad Bennett, (he must not have been a Captain then, he was a Commander, and at that time, he was in charge of Support Services) suggested and authorized that two of everything be fabricated. This was an excellent suggestion because it greatly facilitated the assembly of the apparatus. We had a successful first instrument much more quickly because if one piece didn't work the other one did. Eventually, we had two apparatuses. So, as a result, we had papers with experimental data already analyzed, and in print, barely two years from the time we first started designing the instrument.

A popular slogan in the 40s was "Join the Navy and See the World." I didn't know it applied to civilian scientists, but apparently it did because it turned out that way.

Our subsequent work concerned X-ray diffraction and the elucidation of the three-dimensional structure of molecules. A key problem existed; in fact, half of the necessary information seemed to be lost in the process of the diffraction procedure. It was called the phase problem. If we could evaluate the phases as well as the intensities, then we could work backwards and determine the structures of these molecules. Well, Jerome Karle, with a colleague, Herbert Hauptman, who worked in our group at the time, solved the problem of obtaining the phases theoretically. The results were presented in terms of an infinite set of inequalities, probabilistic functions, and transcendental functions. It was I who bridged the gap between the theory and experiment by translating these mathematical results into practical procedure. Jerome always said he liked working with a paper and pencil much better than anything else. There was a great amount of trepidation when we gambled our research budget to have IBM do a final refinement on my first results. You see, at that time, this was the mid-1950s – IBM was the only company that had a computer that was capable of doing the problem that we needed to be done. Their computer was displayed in New York City on Fifth Avenue behind a plate-glass window, so that passerbys could see this wondrous machine doing its thing. Well, fortunately, their machine worked. My results worked and that was the beginning of doing several hundred (I've not counted them) structures over the years, in various areas of science. The successes we've had, in this sort of activity, have spawned numerous advance-study workshops that took place around the world for the next 20 to 25 years. These are the places I remember; there were a number of others. Cambridge University – I think that was the first one – and then Oxford, York, Parma, Erice (on top of a mountain in Sicily) Prague, Warsaw, Hungary, Kyoto, Brazil and so forth. In that way, we saw the world rather thoroughly. However, I didn't get to the North Pole until two years ago. There were a number of scientists there, and I presented some lectures. I should say that this

was in Tromso, at the university, way up above the Arctic Circle. The notes and instructions that I provided for the workshops became teaching materials in various universities and the basis for a number of computer programs. These courses were instrumental in expanding the number of crystal structures solved around the world, from a handful each year to much more than 10,000 a year, at present. We know how many because these structures are all in a data base called the Cambridge Data Base and they are having a difficult time keeping up with the exponential number of pieces of data that they have to include every year.

Personally, I've had a satisfying and fascinating career. Much of the success is due to sufficient support. At present, with our economy at a lower level, there is a tendency to de-emphasize basic research in many institutions. I would like to mention two recent publications that address the profits of society from basic research. The first is the Physics Today issue. In fact, it's the October 1993 issue that is devoted to the benefits of basic research and some of the titles are: "From Basic Research to High Technology," such research is the seed corn of the technological harvest that sustains modern society; "The Birth of the Laser Era." and "Fiber Optics," these are the components that went into making fiber optics practical. Fundamental research in glass science, optics, and quantum mechanics have matured into a technology that is now driving our communications revolution. Then, of course, there are the magnetic resonance experiments, superconductivity, semiconductors, cyclotrons, and so on and so on. A somewhat similar publication came out recently from the American Chemical Society, under the direction of Ernest

Dr. Isabella and Dr. Jerome Karle with their daughters Madeleine Tawney on the left and Dr. Jean Karle on the right at the ceremony. Another daughter Louise Hanson was not able to attend.

Eliel. It's called Science and Serendipity, and it has a number of fascinating articles on how basic research, that was not directed toward anything, has resulted in nylon, teflon, and the platinum-plated bullet (renamed cisplatin, an anticancer drug). For the medical field, chemistry has provided cortisone, designer genes, AZT, and so on. I have mentioned chemistry and physics. Of course, similar examples exist in medicine and physiology, biology, agriculture and all the other scientific areas. Everywhere we look in modern society we see the end-product of basic research. Often it takes 10 or 50 or even more years for the knowledge derived from basic research to be applied to high technology, but the pool containing basic information must be constantly replenished, otherwise it will run dry.

Again, I want to express my thanks to the Franklin Institute for choosing me as the Bower Award recipient and to the Navy and the Naval Research Laboratory for all of their support for the last 47 years. Thank you. I also want to thank everybody for helping me celebrate tonight.

CAPT Gaffney: Thank you Dr. Karle, Dr. Jones, Mr. Secretary, Dr. Tise, Dr. Powell and especially to the Franklin Institute, today. This is a memorable evening for the Navy, the Naval Research Laboratory and I'm sure for all the Karles that are here. We all look forward to the grand ceremony at the Franklin Memorial in Philadelphia in the spring.

Now, if all of you will help us with the rest of the reception, we'll let the press spend some time with Isabella alone.

Thank you very much everyone.

Molecular Structure: Four Articles

But beyond the bright search lights of science
Out of sight of the windows of sense,
Old riddles still bid us defiance,
Old questions of Why and of Whence.

When Science from Creation's face
Enchantment's veil withdraws,
What lovely visions yield their place
To cold material laws!

Thomas Campbell (1777-1844) – To The Rainbow

The following four articles by Isabella Karle represent three important and distinct areas of science which she developed and which have changed our thinking about the structure of matter. By developing X-ray diffraction techniques for determining the three-dimensional structure of molecules, she has made possible new avenues of research in chemistry, biology and medicine.

The three areas of science and the accompanying articles are:

- Structure analysis of molecules in the vapor state by electron diffraction – "Internal Motion and Molecular Structure Studies by Electron Diffraction," (1949).
- The determination of phases directly from the measured intensities of X-ray reflections – "Crystal and Molecular Structure of p,p'-Dimethoxybenzophenone by the Direct Probability Method" (1957) and "An Application of the Symbolic Addition Method to the Structure of L-Arginine Dihydrate," (1964).
- Elucidation of molecular formulae and determinations of conformations of peptides, steroids, and alkaloids – "Crystal Structure of [Leu]zervamicin, a Membrane Ion-Channel Peptide: Implications for Gating Mechanisms," (1991).

In order to maintain authenticity and accuracy, the four articles have been photographically duplicated as originally printed.

Reprinted from THE JOURNAL OF CHEMICAL PHYSICS, Vol. 17, No. 11, 1052-1058, November, 1949
Printed in U. S. A.

Internal Motion and Molecular Structure Studies by Electron Diffraction*

ISABELLA LUGOSKI KARLE AND JEROME KARLE
Naval Research Laboratory, Washington, D. C.

(Received January 31, 1949)

A procedure has been developed for the determination of molecular structure by electron diffraction which yields accurate intensity data and obviates the necessity for visual examination of the diffraction photographs. The theory for computing radial distribution curves has been extended to permit accurate curves to be obtained from scattering data covering only a restricted range of angle. From this method, it is possible to obtain not only equilibrium distances but also the probability distributions for the vibrational motion between pairs of atoms in a molecule. The procedure has been applied to CCl_4 and CO_2 and when comparisons may be made with spectroscopic results, satisfactory agreement is obtained.

THE study of molecular structures using electron diffraction by gases has usually involved the visual examination of the diffraction pattern[1] which consists of small oscillations about a steeply falling background. The positions of the apparent maxima and minima are measured, their relative intensities are estimated visually, and some estimate is made of the shape of those features which appear to be neither maxima nor minima. The observed curve is used as the basis for evaluating the equilibrium distances in the molecule being studied. This is accomplished by calculating a radial distribution curve which is used as a guide for selecting various models to represent the structure of the molecule. From these models intensity curves are computed and compared to the visually observed curve. The model chosen to represent the structure of the molecule depends upon the agreement between the computed and observed curves. Some differences are found in the form of the functions used by various investigators to compute the radial distribution and intensity curves.

The uncertainties in the visual examination of the diffraction patterns and in the mathematical analysis, make it very desirable to establish a quantitative procedure which uses an unambiguous theory and eliminates the visual study of the photographs. A procedure to eliminate this visual study has been developed by the Norwegian school and they have used it to study the structures of a large number of molecules.[2] Their procedure involves the use of a rotating sector[3] in order to accentuate the oscillating features of the pattern and the photographs are scanned with a microphotometer. The main difference between their procedure and the one to be outlined concerns the method of analyzing the scattering data. By our method accurate values of the equilibrium distances can be expected and, in addition, it is possible to evaluate the magnitude of the vibrational motion between pairs of atoms in a molecule.

THEORY

When free molecules are struck by a beam of fast electrons, part of the scattering of the primary beam arises from the spacings between the atoms in individual molecules and can be represented by the formula

$$I_m(s)=\sum_{i=1}^{n}\sum_{j=1}^{n} c_{ij}A_{ij}. \quad (i\neq j) \qquad (1)$$

The rest of the scattering does not depend upon the molecular structure and forms a steeply falling background upon which the molecular scattering, Eq. (1), is superimposed. The upper limit n in the summation is

* Presented at the meeting of the American Society for X-Ray and Electron Diffraction, Columbus, Ohio, December 16, 1948.

[1] L. O. Brockway, Rev. Mod. Phys. 8, 231 (1936).

[2] (a) Chr. Finbak, Avhandl. Norske Vid.-Akad. Oslo, I Mat.-Naturv. Kl., No. 7 (1941). (b) Chr. Finbak and O. Hassel, Archiv. f. Mat. o. Naturvid. B45, No. 3 (1941). (c) H. Viervoll, Acta Chem. Scand. 1, 120 (1947). (d) O. Hassel and H. Viervoll, Acta Chem. Scand. 1, 149 (1947).

[3] (a) C. Finbak, Avhandl. Norske Vid.-Akad. Oslo, Mat.-Naturv. Kl., No. 13 (1937). (b) P. P. Debye, Physik. Zeits. 40, 66, 404 (1939).

equal to the total number of atoms in the molecule. The coefficients c_{ij} are characteristic of the ith and jth atoms and in the subsequent analysis are assumed to be constant. In practice, this is a good approximation, except for very small scattering angles, if the molecular scattering is obtained by dividing the total scattering by the background scattering. If a molecule is absolutely rigid, then the interference function A_{ij} is equal to $\sin sr_{ij}/sr_{ij}$ where r_{ij} is the distance between the nuclei of the ith and jth atoms and $s=(4\pi \sin\theta/2)/\lambda$ where θ is the scattering angle and λ is the wave-length of the electron beam. Since there is some motion of the nuclei in all molecules, the interference function A_{ij} assumes the form

$$A_{ij}=\int_0^\infty P_{ij}(\rho)(\sin s\rho/s\rho)d\rho, \qquad (2)$$

where $P_{ij}(\rho)d\rho$ is the probability that the distance between the ith and jth atoms has a value between ρ and $\rho+d\rho$.

A Fourier transformation may be made on the molecular scattering function,

$$I_m(s)=\sum_{i=1}^{n}\sum_{j=1}^{n} c_{ij}\int_0^\infty P_{ij}(\rho)(\sin s\rho/s\rho)d\rho, \quad (i\neq j) \qquad (3)$$

by multiplying it by $s\sin sr$ and integrating with respect to s. The result of such a procedure is a function of the variable r which represents the radial distribution curve, $D(r)$;[4]

$$D(r)=\int_0^\infty sI_m(s)\sin sr\,ds \qquad (4)$$

$$=\sum_{i=1}^{n}\sum_{j=1}^{n} c_{ij}\int_0^\infty \sin sr\,ds\int_0^\infty \frac{P_{ij}(\rho)}{\rho}\sin s\rho\,d\rho \qquad (4a)$$

$$=\frac{\pi}{2}\sum_{i=1}^{n}\sum_{j=1}^{n} c_{ij}\frac{P_{ij}(r)}{r}. \qquad (4b)$$

The ordinates of the radial distribution curve essentially represent the probability of the occurrence of the internuclear distances, r, in the molecule. It has been found in our experiments that in the vicinity of an equilibrium distance, r_{ij}, which is not very close in value to other ones in the molecule, the function $D(r)$ can usually be represented by

$$D(r)=c_{ij}(\pi h_{ij})^{\frac{1}{2}}\exp[-h_{ij}(r-r_{ij})^2]/2r_{ij}, \qquad (5)$$

where $(2h_{ij})^{-\frac{1}{2}}$ is a measure of the average deviation from the equilibrium position and is equal to $(l_{ij}^2)^{\frac{1}{2}}$ where l_{ij} is the displacement from equilibrium. The quantity r in the denominator in Eq. (4b) may be replaced by r_{ij} when h_{ij} is sufficiently large.

[4] The derivation follow the treatment by P. Debye, J. Chem. Phys. 9, 55 (1941).

In order to evaluate the integral in Eq. (4), the molecular scattering data must be known to values of s equal to infinity. In practice, only a limited amount of data are available. Nevertheless, this limited data uniquely determines the structure of a molecule. The procedure used is to compute the following modified function,[5]

$$f(r)=\int_0^{s_{max}} sI_m(s)\exp(-as^2)\sin sr\,ds, \qquad (6)$$

where s_{max} bounds the range of scattering data and a can be so chosen that the integrand of Eq. (6) makes no essential contribution beyond s_{max}. The computed $f(r)$ curve, therefore, is the same as that which would have been obtained if s_{max} approached infinity. It is possible then to obtain the desired function, $D(r)$, from $f(r)$ by making use of the relationship[6]

$$f(r)=\frac{1}{2(\pi a)^{\frac{1}{2}}}\int_{-\infty}^{\infty} D(\rho)\exp[-(r-\rho)^2/4a]d\rho, \qquad (7)$$

where a is the same as that used in Eq. (6). The introduction of $D(r)$ as defined in Eq. (5) leads to an evaluation of the integral in Eq. (7), giving for $f(r)$ the expression

$$f(r)=c_{ij}(\pi h_{ij})^{\frac{1}{2}} \times\exp[-h_{ij}(r-r_{ij})^2/(4ah_{ij}+1)]/2r_{ij}(4ah_{ij}+1)^{\frac{1}{2}}. \qquad (8)$$

In practice, the bell-shaped peaks which result from the computation of Eq. (6) are curve fitted by the function, $B_{ij}\exp[-H_{ij}(r-r_{ij})^2]$, where $H_{ij}=h_{ij}/(4ah_{ij}+1)$ (see the exponent in Eq. (8)). Since a is the value used in computing Eq. (6), h_{ij} can be readily obtained. The values of h_{ij} so determined, as pointed out, are the measure of the magnitude of the vibrational motion between pairs of atoms in a molecule.

Equation (8) may be used to illustrate the unique determination of the function, $D(r)$, from a limited amount of data. By this we mean in a mathematical sense that the data may be extended uniquely beyond its experimentally determined range. There is, of course, always some uncertainty in experimental data. In a practical sense, then, it is possible to extend a function on the basis of a uniqueness property in a definite fashion beyond its known experimental range, but the uncertainties in the experiment will introduce some uncertainty into the extension. There is a unique relation between the function in Eq. (8) whose parameters may be determined from experiment and the desired function in Eq. (5). If h_{ij} and r_{ij} are evaluated by applying Eq. (8) to a computed curve, then $D(r)$ is a known numerical function of r. From one rather re-

[5] The damping factor $\exp(-as^2)$ was introduced by Degard in order to improve radial distribution calculations. See C. Degard, Bull. Soc. Roy. Sci. Liege 12, 383 (1937). The effect of this and other damping factors on radial distribution curves has been studied by J. Waser, Thesis, California Institute of Technology.

[6] E. C. Titchmarsh, *Introduction to the Theory of the Fourier Integral* (Clarendon Press, Oxford, 1937), p. 51.

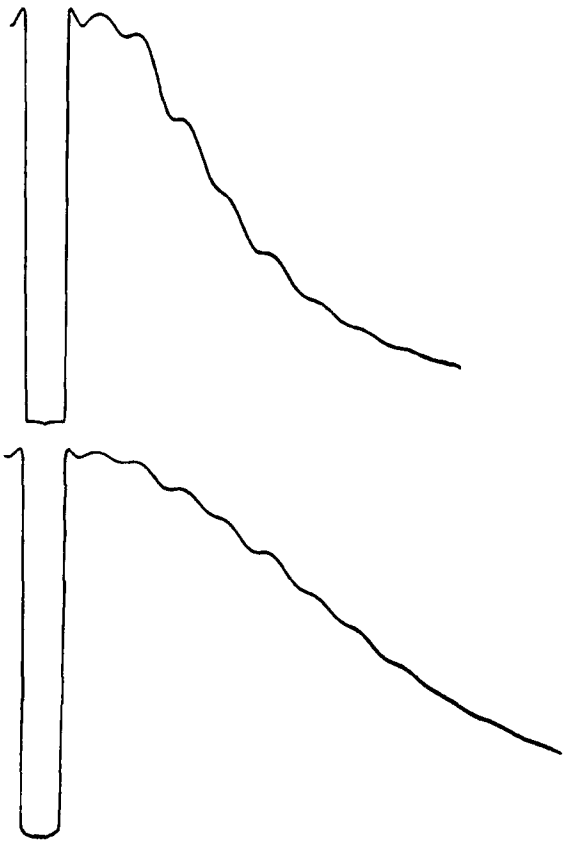

FIG. 1. Typical microphotometer traces of a light and medium exposure of CCl_4. The vertical scales are not the same.

stricted, but simple, point of view, this uniqueness can be based upon the theoretical result[7] that the computed radial distribution curve can be represented by the sum of Gaussian distributions. From another point of view, the study of the mathematics of positive Fourier integrals shows that the scattering function, $I(s)$, known only in a restricted range of angle is related within narrow bounds to only one positive distribution function. This idea has been used in our laboratory to improve the accuracy of determining electron distributions[8(a)] about atoms. The restrictiveness of positive functions has also been found useful for small angle scattering and in the evaluation of the phases of the Fourier coefficients in the determination of crystal structure.[8(b)]

In the case of gas molecules, though, it is not necessary to resort to powerful mathematical arguments to obtain accurate information from a restricted amount of data. If the experimental curve, $f(r)$, is merely fit well by a function in the vicinity of r_{ij} (though the function may even become negative at some larger distance), a good evaluation of the desired $D(r)$ in the vicinity of r_{ij} can be obtained. This may be seen from Eq. (7) which shows that for values of a usually used (0.005–0.010), the exponential function is practically a delta-function so that $f(r)$ is merely a smeared or broadened version of $D(r)$. The main contribution of the integrand of Eq. (7) is in the vicinity of $\rho=r$.

The radial distribution curve yields three kinds of information; the equilibrium interatomic distances, an evaluation of the vibrational motion between pairs of atoms, and the coefficients for the molecular scattering expression which are related to the areas under the peaks. The structures of many molecules can be completely determined from radial distribution calculations alone. If several interatomic distances in a molecule fall close together, however, the information obtainable from a radial distribution curve is restricted and should be supplemented by additional data which can be obtained from computed intensity curves. The formula to be used is

$$I_m(s)=\sum_{i=1}^{n}\sum_{j=1}^{n} c_{ij}\exp(-s^2/4h_{ij})\sin sr_{ij}/sr_{ij} \quad (i\neq j), \quad (9)$$

where the values of c_{ij}, h_{ij}, and r_{ij} for various models are chosen to be consistent with the data available from the radial distribution curve. Equation (9) has been obtained by James[7] by integrating Eq. (3), using a probability distribution function which is derived on the basis of Hooke's law forces.

PROCEDURE

The diffraction photographs were taken with an electron diffraction camera which has been constructed recently in our laboratory. The accelerating voltage usually used is about 40,000 volts and is regulated to about one volt in 10,000. The voltage can be read continuously on a Type K potentiometer. The voltage obtained from the measurement of diffraction rings on a gold photograph agrees to within 0.1 percent with that read on the potentiometer. The electron beam is focused by a focusing grid and two magnetic lenses. The beam passes through a defining aperture of 0.1 mm diameter and is essentially parallel between the aperture and the photographic plate.

A rotating sector is incorporated in the specimen chamber. The sector is attached to a ball-bearing race six inches in diameter which is rotated by a synchronous motor using a friction drive. The motor is in the specimen chamber and its operation does not affect the vacuum nor the electron beam. When the sector reaches a speed of 1300–1400 r.p.m., the motor is turned off and pulled away from the race. The speed decreases to about 800 r.p.m. in five seconds during which time an exposure is made. An s^3 sector which is cut to operate between s values of one and 35 has been used so far. The portion between s values of zero to one acts as a beam stop. In order to facilitate the centering of the sector with respect to the electron beam, a speck of fluorescent material is placed in a 0.1-mm diameter

[7] R. W. James, Physik. Zeits. 33, 737 (1932).
[8] (a) H. Hauptman and J. Karle, submitted to Phys. Rev. (b) J. Karle and H. Hauptman, submitted to Acta Cryst.

hole bored in the center of the sector. Photographs of the beam using this arrangement show that there is no correction for fogging required for the exposure times ordinarily used.

The diffraction patterns obtained on contrast lantern slides are traced on a Leeds and Northrup microphotometer. During the tracing they are rotated rapidly[9] in order to average out any irregularities caused by graininess. Care is taken to set the zero of the microphotometer on an unexposed portion of the plate. Traces obtained by this procedure are shown in Fig. 1. The microphotometer readings are calibrated to read electron intensities by taking several series of transmission photographs of evaporated gold on Formvar for various exposure times. The results of such a procedure are easily interpreted since the reciprocity law holds for fast elections,[10] that is, the exposure is equal to the product of the intensity and the time. The gold photographs are taken using the rotating sector and are rotated during the tracing in order to duplicate as closely as possible the procedure used with the gas photographs. A typical calibration curve is illustrated in Fig. 2.

The microphotometer readings are converted to intensity readings which are plotted against the variable s and a smooth background is drawn through the oscillations.[11] It usually is easier to draw the background line beyond s values of 5 or 6 if the experimental intensity curve is multiplied by s or s^2 to accentuate the oscillations about the background. In this respect

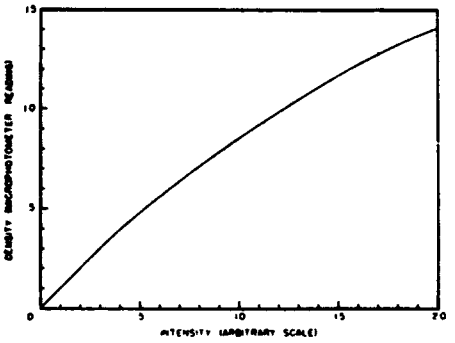

FIG. 2. Typical calibration curve for converting microphotometer readings to electron intensities.

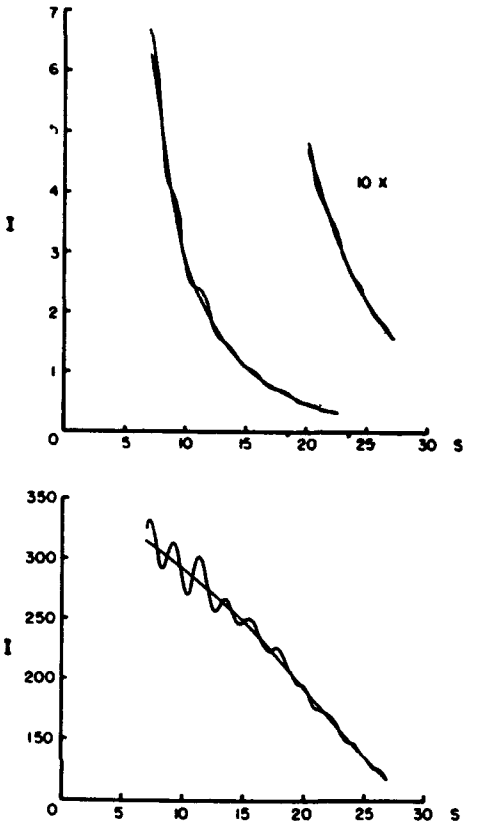

FIG. 3. The upper curve represents the intensity obtained from a fairly dark photograph of CCl_4 taken with an s^3 sector. The lower curve represents the intensity from the upper curve multiplied by s^3. Background curves are drawn through the oscillations.

our experiments would probably have been aided by the use of a sector cut to a power of s higher than 2. Figure 3 illustrates how the background line was drawn for an intensity curve from a photograph of CCl_4 whose useful density range covers values from seven to 27. The molecular scattering is obtained by dividing the experimental intensity by the background curve. This procedure not only eliminates the background scattering but replaces by constants, except at low s values, the variable coefficients in the molecular scattering expression. It is possible to measure the intensity of molecular scattering to much higher accuracy than may be implied by the inaccuracies in determining the absolute intensity. The inaccuracy in absolute measurement may be greater than the magnitude of an oscillation at the larger scattering angles. However, molecular intensity measurements concern the magnitude of an oscillation relative to a background line. The accuracy is therefore determined by the amplitude of an oscillation rather than by the measurement of total photographic intensity. Five photographs ranging from light to heavy exposures were used to obtain the molecular scattering curves. The uppermost curves in Figs. 4 and 5 are the experimental molecular scattering curves for CCl_4 and CO_2. The upper curve in Fig. 5 shows the

[9] Karle, Hoober, and Karle, J. Chem. Phys. 15, 765 (1947).

[10] (a) A. Becker and E. Kipphan, Ann. d. Physik (5) 10, 15 (1931). (b) W. Bothe, Zeits. f. Physik 8, 243 (1922).

[11] Uncertainties in the position of the background line affect mainly the shapes but not the positions of the maxima in the radial distribution curve. Hence, fairly reliable equilibrium distances in a molecule can be obtained from the first computation of a radial distribution curve and an intensity curve based on these distances may be computed. The background line may then be corrected if necessary to correspond to the position of the zero axis in the intensity curve provided that no sudden changes occur in curvature of this line. This procedure may be repeated until it is evident that no additional improvement is possible. The improvement in the position of the background line should ordinarily be accompanied by a decrease in the magnitude of the negative portions of the radial distribution curve. Ideally, the radial distribution curve should be positive.

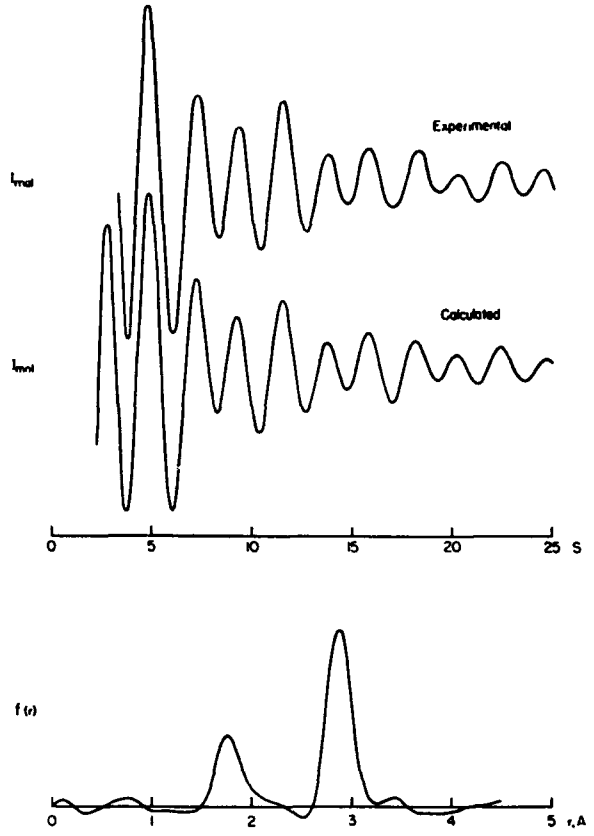

FIG. 4. The three curves represent the experimental molecular scattering, the calculated molecular scattering, and the radial distribution for CCl_4. The vertical scales for the molecular scattering curves are the same.

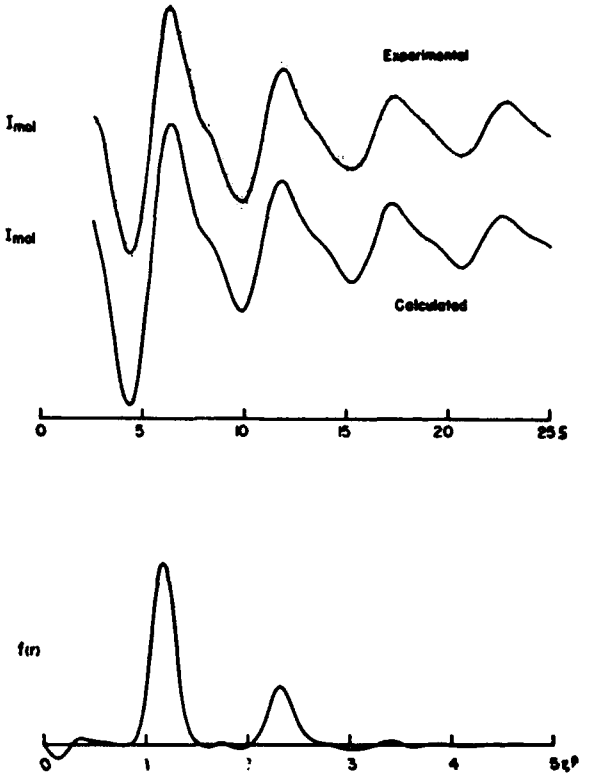

FIG. 5. The three curves represent the experimental molecular scattering, the calculated molecular scattering, and the radial distribution for CO_2. The dots in the upper curve are the experimental points obtained in five independent experiments. Many of the points lie on the curve itself. The vertical scales for the molecular scattering curves are the same.

spread of experimental points for CO_2. The magnitudes of the maxima and minima in this experimental curve are known to within five percent. The characteristic asymmetry in the maxima and minima is well defined.

A radial distribution curve is calculated using the experimental data. The integral in Eq. (6) is replaced by a summation where the s interval is 0.2. For the CCl_4 and CO_2 computations, maximum s was 25 and a was chosen to be 0.0057. The calculations were performed with the aid of punched cards and I.B.M. machines.[12] In the experimental intensity curve there is no useful data below s values of two and the region below s values of three or four does not represent a molecular scattering curve with constant coefficients. Hence, the region between s values of zero to three or four is replaced by an intensity curve computed with constant coefficients from an assumed model. If this model is inconsistent with the results of the radial distribution calculation, the calculated portion of the intensity curve is adjusted and a new radial distribution curve is computed. With this method of successive approximations, relatively few calculations need be made. The radial distribution curve should consist of a series of positive peaks, since the scattering from the electronic shells of the atoms has been eliminated. The radial distribution curves for CCl_4 and CO_2 are illustrated in Figs. 4 and 5.*

Each peak of the radial distribution curve is fitted with the function $B_{ij}\exp[-h_{ij}(r-r_{ij})^2/(4ah_{ij}+1)]$, Eq. (8), to obtain h_{ij} and r_{ij} values. Only the upper two-thirds of a peak is used in order to minimize the effect from small oscillations in the base line. Relative values of the coefficients c_{ij} which are used in the calculated intensity curves can be obtained in two ways; (a) each c_{ij} value is proportional to the area under its corresponding peak multiplied by the equilibrium distance associated with that peak, or (b) the maximum value of the peak, B_{ij}, is proportional to $c_{ij}(h_{ij})^{\frac{1}{2}}/r_{ij}(4ah_{ij}+1)^{\frac{1}{2}}$. Using the experimental h_{ij}, r_{ij}, and c_{ij} values, theoretical intensity curves were computed for CCl_4 and CO_2

[12] Shaffer, Schomaker, and Pauling, J. Chem. Phys. 14, 659 (1946).

* *Note added in proof.*—Recent investigations in our laboratory on more complicated molecules have demonstrated that extraneous oscillations such as those which appear in the f(r) curves of Figs. 4 and 5 can be considerably reduced by readjusting the background line in the total intensity curves. It has also been found that a peak in the radial distribution curve formed from several interatomic distances may be decomposed into its components which yield directly the detailed structure of the molecule. Computed molecular intensity curves are used mainly to establish the range of uncertainty.

using Eq. (9). As expected, these were found to agree very well with the experimental curves (Figs. 4 and 5). In this instance, the calculated intensity curves merely illustrate the consistency of the procedure. On the other hand, when there are structural features that are not resolved in the radial distribution curve, more emphasis will have to be placed on theoretical intensity curves.

RESULTS

The experimental results are listed in Table I. For CO_2, the C−O distance compares favorably with the spectroscopic result of 1.163A for the equilibrium value. The experimentally determined values for the O−O distance is not exactly double the value for the C−O distance. This deviation, however, falls within the experimental uncertainty. The average amplitude of the vibrations of the C−O bond was calculated from spectroscopic data using the expression[4]

$$l^2 = 1/2h = (\mu_1 + \mu_2)/2\alpha, \tag{10}$$

where α is the force constant between the C and O atoms and μ is the average energy of an oscillator given by Planck's expression, $\mu = h\nu/2 + h\nu/(\exp(h\nu/\beta T) - 1)$. The expression for the O−O distance is

$$l^2 = \mu_1/\alpha. \tag{11}$$

The numerical values used were $\alpha = 15.5\times10^5$ dynes cm^{-1}, $\nu_1 = 4.0\times10^{13}$ sec.$^{-1}$, and $\nu_2 = 7.0\times10^{13}$ sec.$^{-1}$.[13] The electron diffraction value for $(l^2)^{\frac{1}{2}}$ for the C−O distance agrees well with the spectroscopic value. The difference between the electron diffraction and the spectroscopic values of $(l^2)^{\frac{1}{2}}$ for the O−O distance may be attributed mainly to the fact that the O−O peak in the radial distribution curve is small which makes the determination less accurate. In addition, it should be noted that the spectroscopic value is computed from a simplified theory (Eq. (11)).

There are no spectroscopic values for the interatomic distances in CCl_4 available for comparison. Our values may be compared with other electron diffraction determinations. Finbak and Hassel[2(b)] obtained 1.770A and 2.876A for the C−Cl and Cl−Cl distances using their sector method. Pauling and Brockway[14] obtained 1.76A and 2.87A for the C−Cl and Cl−Cl distances using the visual method. The spectroscopic values for the vibrational motion between the C−Cl and Cl−Cl pairs listed in Table I have been computed by James[7] using the central force model. Rosenthal[15] has shown that CH_4 is the only tetrahedral molecule to which the central force model is applicable. By applying a general force field to tetrahedral molecules, Rosenthal[16] obtained a value of 3.6×10^5 dynes cm^{-1} for the C−Cl force constant in CCl_4. This is larger than the value 2.0×10^5 dynes cm^{-1} used by James and implies that the amplitude for the vibrational motion obtained by James is too large. Better agreement between the electron diffraction and spectroscopic e[illegible]ions of the vibrational motion can be expected [illegible]e from a recalculation of the spectroscopic valu[illegible]ased on the more general force model for CCl_4.

TABLE I.

	r_{ij}(A)	$(\bar{l}_{ij}^2)^{\frac{1}{2}}_{\text{elec. diff.}}$	$(\bar{l}_{ij}^2)^{\frac{1}{2}}_{\text{spect.}}$
	CCl_4		
C−Cl	1.770±0.010	0.041±0.005	0.055
Cl−Cl	2.877±0.020	0.054±0.005	0.071
	CO_2		
C−O	1.162±0.010	0.034±0.003	0.034
O−O	2.310±0.020	0.040±0.007	0.029

It should be mentioned that even very small vibrations like those found in CCl_4 and CO_2 damp the intensity of molecular scattering considerably. For CCl_4 the intensity at s equal to 25 is 60 percent less than it would be for a rigid structure while for CO_2 the intensity is 35 percent less.

The c_{ij} values were obtained from the radial distribution peaks using the methods given above. For CO_2 the value found for the ratio c_{C-O}/c_{O-O} is 1.50±0.02. This value may be compared to the ratio $2Z_CZ_O/Z_OZ_O$ which also is equal to 1.50. Z_C and Z_O are the atomic numbers of carbon and oxygen. For CCl_4 the experimental values of the ratio c_{Cl-Cl}/c_{C-Cl} is 4.22±0.04 whereas the ratio $3Z_{Cl}Z_{Cl}/2Z_CZ_{Cl}$ equals 4.25. These figures indicate that the scattering factors of the atoms involved have about the same shape and that their variability with respect to the angle variable s can be eliminated by dividing the total scattering by the background scattering.

An approximation was made in Eq. (5) by replacing the variable r in the denominator by the equilibrium distance r_{ij}. The effect of this approximation on the determination of the equilibrium distances is very small. The correction is equal to $1/2h_{ij}r_{ij}$ and amounts to not more than 0.001A for the CO_2 and CCl_4 molecules. There is a negligible effect on the shape of the peak.

DISCUSSION

The results on CCl_4 and CO_2 indicate that accurate intensity data can be obtained from electron diffraction investigations of gases. This is borne out by the results in Table I and also by the fact that the radial distribution curves are essentially positive. Relatively little error in the experimental intensity can yield large negative fluctuations in the radial distribution curves. By the procedure described above the magnitude and shape of the various features of the diffraction pattern can be reliably determined, thus minimizing considerably the uncertainties which are bound to arise in the visual examination of the diffraction photographs. The

[13] G. Herzberg, *Infra-Red and Raman Spectra of Polyatomic Molecules* (D. Van Nostrand Company, Inc., New York, 1945), p. 173.
[14] L. Pauling and L. O. Brockway, J. Chem. Phys. 2, 867 (1934).
[15] J. Rosenthal, Phys. Rev. 46, 730 (1934).
[16] J. Rosenthal, Phys. Rev. 49, 535 (1936).

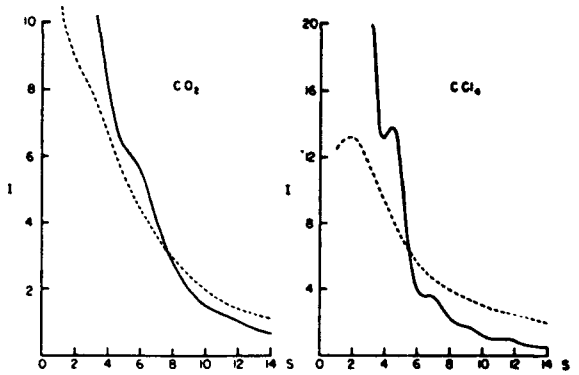

FIG. 6. The solid lines are the experimental scattering curves obtained with an s^3 sector for CCl_4 and CO_2. The dotted lines represent the background scattering calculated from tabulated values and multiplied by s^3.

visual method can be used with confidence to determine the equilibrium distances in a molecule if the diffraction pattern consists of well-defined maxima and minima and if the determination can be based mainly on the positions of these maxima and minima. When the determination of a molecular structure depends upon the relative intensities of the maxima and minima or upon special features such as shelves or asymmetries, the results from the visual method may be considerably less reliable.

There is sufficient difference between the procedure developed by the Norwegian school and the one presented here to merit some comment. In their analysis of the diffraction data, the molecular scattering curve is obtained using the expression[2(c)]

$$I_m(s)=K\left[\frac{P_t(s)}{P_a(s)}-1\right]\left[\frac{\sum_i(Z_i-F_i)^2+\sum_i S_i}{s^4}\right], \quad (12)$$

where $P_t(s)$ is the density reading on a microphotometer trace of a diffraction photograph, $P_a(s)$ is the background curve drawn on this trace to represent the atomic scattering, and $[\sum_i(Z_i-F_i)^2+\sum_i S_i]/s^4$ is the coherent plus incoherent atomic scattering where Z_i is the atomic number, F_i is the atomic scattering factor for x-rays, and S_i is the incoherent scattering function tabulated by Bewilogua.[17] Our procedure differs in that the molecular scattering function with constant coefficients is obtained from the expression

$$I_m(s)=K\left[\frac{I_t(s)}{I_a(s)}-1\right], \quad (13)$$

where the photographic density readings have been converted to intensity readings. In addition, we do not reintroduce the variable scattering factors once they have been eliminated by dividing by the background. The disadvantage of using Eq. (12) for the molecular scattering function is that a proper Fourier inversion cannot be made on an intensity function whose coefficients (corresponding to the c_{ij} in Eq. (4a)) are functions of s. The use of Eq. (12) in a Fourier transform affects the accuracy of determining the equilibrium distances in a molecule very little. However, it is not possible to use such a curve for the evaluation of the vibrational motion in a molecule.

The background scattering merits some discussion. It has always been considered that the background scattering in electron diffraction patterns of gases can be represented by

$$I_a(s)=(K/s^4)[\sum_i(Z_i-F_i)^2+\sum_i S_i]. \quad (14)$$

The results of our experiments are shown in Fig. 6 where the dotted lines represent Eq. (14) calculated from tabulated values and multiplied by s^3, and the solid line is the experimental scattering obtained with an s^3 sector for CCl_4 and CO_2. Theoretically, the solid line should oscillate about the dotted line. The same type of discrepancy is apparent from the examination of published microphotometer traces by the Norwegian school[2] and by Yearian and Barss.[18] Experiments on the scattering from free atoms have been performed and are being continued to establish with certainty that the shape of the background is not a result of some error in the technique of performing the diffraction experiment. The consistency obtained in our experiments to date indicates that the theory of the background scattering may be incorrect. It is obvious, however, from the procedure described in this paper that it is not necessary to have a theoretical expression for the background scattering for the determination of molecular structures.

We wish to thank Professor V. Schomaker of the California Institute of Technology for making available to us a set of punched cards developed in his laboratory for performing electron diffraction computations. We also wish to thank the Naval Ordnance Laboratory for making available their mechanized analysis facilities and the Washington Office of the International Business Machine Corporation for their fine cooperation.

[17] L. Bewilogua, Physik. Zeits. 32, 740 (1931).

[18] H. J. Yearian and W. M. Barss, J. App. Phys. 19, 700 (1948).

Reprinted from *Acta Crystallographica*, Vol. 11, Part 4, April 1958

PRINTED IN DENMARK

Acta Cryst. (1958). **11**, 257

Crystal and Molecular Structure of *p,p'*-Dimethoxybenzophenone by the Direct Probability Method

BY I. L. KARLE, H. HAUPTMAN, J. KARLE AND A. B. WING

U.S. Naval Research Laboratory, Washington, D.C., U.S.A.

(*Received* 29 *August* 1957)

The structure of *p,p'*-dimethoxybenzophenone has been determined from X-ray single-crystal data. The space group is $P2_1/a$ and there are eight molecules in the unit cell. The cell parameters are $a = 16{\cdot}43$, $b = 16{\cdot}03$, $c = 9{\cdot}62$ Å, $\beta = 100° 15'$. The phases of the largest 270 normalized structure factors, $E_{\mathbf{h}}$, were determined directly by probability methods (Hauptman & Karle). A Fourier map with these $E_{\mathbf{h}}$ as coefficients revealed the structure, which was improved by the least-squares method. A line connecting the methoxy oxygens within a molecule is almost parallel to the *b* axis and a second molecule is shifted by approximately $\frac{1}{2}c$ from the first, except that the corresponding benzene rings of the adjacent molecules are twisted in opposite directions. The methyl carbons lie almost in the planes of the adjacent benzene rings.

Also included in this paper is a discussion of the limitations of Σ_1 for $P2_1/a$ and the theoretical basis for the use of an *E* map.

1. Introduction

By this time several structures have been determined using the direct probability method presented in Monograph I (Hauptman & Karle, 1953). Christ, Clark & Evans (1954) have found the structure of colemanite and Christ & Clark (1956) have found the structure of meyerhofferite. Bertaut & Blum (1956) have derived the forms for Σ_1, Σ_2 and Σ_3 of Monograph I appropriate to the space group *Bbmm*, and have applied them to solving the structure of Ti_2CaO_4.

Vand & Pepinsky (1953) purported to demonstrate the failure of the methods based on the joint probability distributions of Monograph I by means of a simple planar four-atom structure. However, Bertaut (1955), using the probability formulas appropriate to the correct space group, *p4m*, easily obtained the true structure, thus nullifying the claim based on this four-atom problem.

The X-ray structure analysis of *p,p'*-dimethoxybenzophenone,

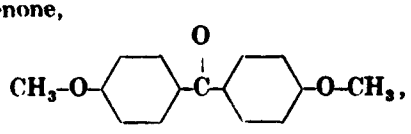

the most complex structure thus far studied by direct probability methods, is described in this paper. Signs for the largest normalized structure factors (E) were determined directly from the magnitudes of the intensities alone by the probability methods of Monograph I. These signs were used to compute a three-dimensional E map, which revealed the structure immediately. The coordinates obtained from this map were then improved using a three-dimensional least-squares procedure. A note concerning this structure has been published by us (Karle, Hauptman, Karle & Wing, 1957).

2. Experimental measurements

The crystals used in this investigation were grown by Mr C. E. Miller of Bell Telephone Laboratories. Dr S. Geller suggested that we apply the probability methods to this material and supplied us with crystallographic data and preliminary diffraction photographs.

The crystals were colorless, opaque needles with the *c* axis as the needle axis. The dimensions of the unit cell were obtained from rotation and Weissenberg photographs. The crystallographic data are:

$$a = 16{\cdot}43,\ b = 16{\cdot}03,\ c = 9{\cdot}62 \text{ Å},\ \beta = 100° 15',$$
$$\text{space group } P2_1/a,\ Z = 8,$$
$$\varrho(\text{X-ray}) = 1{\cdot}289,\ \varrho(\text{physical}) = 1{\cdot}259.$$

There are 30 carbon atoms, 6 oxygen atoms, and 28 hydrogen atoms in general positions in an asymmetric unit.

Equi-inclination Weissenberg photographs were taken about the three crystallographic axes, using nickel-filtered copper radiation. Five exposure sequences were made of each layer. The intensities were estimated visually, using a calibrated comparison strip, and corrections were made for Lorentz and polarization factors, obliquity, α_1, α_2 resolution and spot size (Wing & Birks, 1954). 5527 independent reflections were measured, almost the entire copper sphere, of which 1261 intensities were observed to be zero. The data were corrected for vibrational motion and placed on an absolute scale by means of a K curve (Karle & Hauptman, 1953; see also Wilson, 1949), thus giving $F_{\mathbf{h}}^2$. From these, the magnitudes of the normalized structure factors were computed by means of

$$E_{\mathbf{h}}^2 = F_{\mathbf{h}}^2/\varepsilon \sum_{j=1}^{N} f_{j\mathbf{h}}^2, \qquad (2{\cdot}1)$$

where, for space group $P2_1/a$, $\varepsilon = 2$ when **h** is *h*0*l* or 0*k*0 and $\varepsilon = 1$ otherwise, N is the number of atoms in the unit cell, and f_j is the atomic scattering factor of the jth atom.

The theoretical probability distribution of a structure factor in a centrosymmetric crystal predicts 32% of all $|E| > 1$, 5% of all $|E| > 2$, and 0·3% of all $|E| > 3$. The actual distribution of $|E|$ for this crystal was found to be 25% greater than 1, 6% greater than 2 and 1·4% greater than 3. Theoretically, for a centrosymmetric crystal the following averages occur:

$$\langle|E|\rangle = 0{\cdot}798,\ \langle E^2\rangle = 1{\cdot}0 \text{ and } \langle|E^2-1|\rangle = 0{\cdot}968\,.$$

For this crystal the values for these averages were:

$$\langle|E|\rangle = 0{\cdot}675,\ \langle E^2\rangle = 0{\cdot}986, \text{ and } \langle|E^2-1|\rangle = 1{\cdot}17\,.$$

3. Determination of the phases

Sign determination by the probability formulas in Monograph I* requires only the knowledge of the space group, and the magnitudes of the normalized structure factors. The chemical composition of the unit cell, although useful, is not required for the structure determination. To facilitate the determination of the phases, the E_{hkl} were arranged in order of descending E magnitudes in groups where the indices were *g*0*g*, 0*g*0, *ggg*, *ggu*, *guu*, *gug*, *ugu*, *ugg*, *uug*, and *uuu* (g = even, u = uneven). The E^2-1 values were also listed. It was immediately apparent from the E values that the reflections with l even were considerably stronger than those with l odd. Furthermore, in the groups *ggg* and *ugu* the reflections with $k=4,8,12,\ldots$ were much stronger than those with $k = 2, 6, 10, \ldots$ and in the groups *ugg* and *ggu* all the strong reflections had $k = 2, 6, 10, \ldots$. There was no particular pattern for k odd. Since an ordered distribution of normalized intensities (E^2) with respect to the k index existed for this crystal, it was necessary to examine the effect it would have on the phase-determining formulas.

The square of the normalized structure factor for $P2_1/a$ for the case of equal atoms is

$$\begin{aligned} E^2_{hkl} &= F^2_{hkl}/\sum_{j=1}^{N} f_j^2 \\ &= \frac{16}{N}\sum_{j=1}^{N/4}\cos^2 2\pi(hx_j+lz_j)\frac{\cos^2}{\sin^2}2\pi ky_j \\ &+ \frac{16}{N}\sum_{j\neq j'}^{N/4}\cos 2\pi(hx_j+lz_j)\frac{\cos}{\sin}2\pi(hx_{j'}+lz_{j'}) \\ &\times \frac{\cos}{\sin}2\pi ky_j\frac{\cos}{\sin}2\pi ky_{j'}\,, \end{aligned} \tag{3·1}$$

where the cosine terms apply to the case where $h+k$ is even and the sine terms to $h+k$ odd. Using various trigonometric relations, (3·1) can be rewritten in the form

$$E^2_{hkl}-1 = (-1)^{h+k}\frac{1}{N^{\frac{1}{2}}}E_{2h,0,2l}+R \tag{3·2}$$

or

$$(-1)^{h+k}(E^2_{hkl}-1) = \frac{1}{N^{\frac{1}{2}}}E_{2h,0,2l}+(-1)^{h+k}R\,, \tag{3·3}$$

where

$$\begin{aligned} R = \frac{4}{N}\sum_{j=1}^{N/4}&[(-1)^{h+k}+\cos 4\pi(hx_j+lz_j)]\cos 4\pi ky_j \\ &+\frac{4}{N}\sum_{j\neq j'}^{N/4}\{(-1)^{h+k}\cos 2\pi[h(x_j+x_{j'})+l(z_j+z_{j'})] \\ &+\cos 2\pi[h(x_j-x_{j'})+l(z_j-z_{j'})]\} \\ &\times\{(-1)^{h+k}\cos 2\pi k(y_j+y_{j'})+\cos 2\pi k(y_j-y_{j'})\}\,. \end{aligned}$$

Upon averaging over the index k, expressions (3·2) and (3·3) become

$$\langle E^2_{hkl}-1\rangle_k = \langle R_1\rangle_k+\langle R_2\rangle_k+\langle R_3\rangle_k \tag{3·4}$$

and

$$\langle(-1)^{h+k}(E^2_{hkl}-1)\rangle_k = \frac{1}{N^{\frac{1}{2}}}E_{2h,0,2l}+\langle R_4\rangle_k+\langle R_5\rangle_k+\langle R_6\rangle_k \tag{3·5}$$

where we find, for example,

$$\langle R_1\rangle_k = \frac{4}{N}\sum_{\nu\neq\nu'}^{N/4}\cos 2\pi[h(x_\nu-x_{\nu'})+l(z_\nu-z_{\nu'})]\,, \tag{3·6}$$

$$\langle R_4\rangle_k = \frac{4}{N}\sum_{\nu\neq\nu'}^{N/4}\cos 2\pi[h(x_\nu+x_{\nu'})+l(z_\nu+z_{\nu'})]\,, \tag{3·7}$$

and the indices ν and ν' range over those values of $j = 1, 2, \ldots, N$ for which $y_\nu - y_{\nu'} = 0$, ($y_\nu \neq 0$ or $\frac{1}{2}$). In other words, the subscripts ν, ν' refer only to those pairs of atoms whose y coordinates ($\neq 0$ or $\frac{1}{2}$) are the same. Similar expressions are obtained for $\langle R_2\rangle_k$ and $\langle R_5\rangle_k$ with $y_\nu+y_{\nu'} = 0$ ($y_\nu \neq 0$ or $\frac{1}{2}$) and for $\langle R_3\rangle_k$ and $\langle R_6\rangle_k$ with $y_\nu = y_{\nu'} = 0$ or $\frac{1}{2}$. In the general case where $y_\nu \neq \pm y_{\nu'}$ and $y_\nu \neq 0$ or $\frac{1}{2}$, then all the remainder terms $\langle R_n\rangle_k$ reduce to zero. Consequently, in the general case, the value of (3·4) is zero, and (3·5) becomes the phase-determining formula Σ_1 for $P2_1/a$ (Hauptman & Karle, 1953). Obviously, if many pairs of atoms in the asymmetric unit have the same y coordinate or are in the planes $y = 0$ or $\frac{1}{2}$, the remainder term in (3·5) can become significant and the signs for $E_{2h,0,2l}$ determined from Σ_1 may not be reliable.

An estimate of the feasibility for using Σ_1 in $P2_1/a$ can be made from the value of the quantity $\langle|\langle E^2_{hkl}-1\rangle_k|\rangle_{h,l}$, which is first averaged over k for fixed h, l and then over all h, l. If the y coordinates of the atoms are not equal to 0 or $\frac{1}{2}$ or to each other, then the above quantity should have a value near zero. Deviations from zero are expected since a finite number of data are used in the averages. In this crystal, however, the value of the average was 0·608, two to three times the value to be expected from the size of sample used if the magnitudes of no two y

* Since the solution of this crystal structure, more powerful phase-determining formulas have been derived (see Hauptman & Karle, 1957, 1958 and Karle & Hauptman, 1957, 1958).

coordinates were identical. Thus the conditions for the exact validity of Σ_1 for $P2_1/a$ were not fulfilled. Therefore, the use of this formula would require the establishment of a high level of rejection, i.e. a sign would be accepted only if the value of Σ_1 were unusually large when compared with its standard deviation. As it turned out, the values of Σ_1 for $P2_1/a$ were sufficiently large for only three of the E_{y0y}, the magnitudes of which were too small to be useful in the early stages of the phase-determining procedure. Accordingly Σ_1 for $P2_1/a$ was not useful, and it was decided to treat the crystal as if it were in $P\bar{1}$.

A similar analysis can be made for the Σ_1 formula for $E_{0,24,0}$ in which case atoms having both the same x and z coordinates introduce a limitation. For this crystal the value of $\langle|\langle E^2_{hkl}-1\rangle_{h,l}|\rangle_k$ was 0·221, a value several times larger than that expected from the number of terms in this average. Accordingly, only one sign was determined using this formula, $E_{0,12,0}=-2{\cdot}41$. As it happened this sign was not useful in the earlier stages of the phase determination, but later on played the role of corroborating phases obtained otherwise.

The Σ_1 formula in space group $P\bar{1}$ is not subject to the same limitations as Σ_1 in $P2_1/a$. Therefore the initial phases from which the rest of the phases were obtained were determined using Σ_1 for $P\bar{1}$,

$$sE_{2\mathbf{h}} \sim s(E^2_{\mathbf{h}}-1)\,, \qquad (3{\cdot}8)$$

where s symbolizes 'sign of' and $\sim$ means 'probably is'. Here a phase is determined only from the magnitude of one other reflection. In order to have a high probability that the phase indication is correct, it is necessary that both $E_{2\mathbf{h}}$ and $E^2_{\mathbf{h}}-1$ have large magnitudes. Since the largest negative value that E^2-1 can have is -1, whereas the positive values can be much greater than $+1$, only positive signs are obtained with Σ_1 in a structure of this complexity. For this crystal, signs for four reflections were accepted with this formula. They are listed in Table 1.

$P_{(+)}(E_{2\mathbf{h}})$ indicates the probability that a particular sign is positive. Values in column (a) were computed from the hyperbolic tangent formula of Woolfson (1954) and those in column (b) from (3·29) in Monograph I. Both formulas give approximate values of the probability but they are sufficiently accurate to indicate whether a sign should be accepted. A more accurate value of the probability can be obtained by taking higher-order approximations in deriving the joint probability (see (3·03) and p. 43 in Monograph I).

Next, formula Σ_3 was used to expand the table of signs,

$$sE_{2\mathbf{h}} \sim s\sum_{\mathbf{k}} E_{2\mathbf{k}}(E^2_{\mathbf{h}+\mathbf{k}}-1)\,. \qquad (3{\cdot}9)$$

In this formula, the signs of several $E_{2\mathbf{k}}$ must be known in order to determine the sign of an $E_{2\mathbf{h}}$. Again, only reflections with large E values are examined so that the probability of assigning a correct sign is high. An example of applying Σ_3 to find the sign of $E_{\bar{1}\bar{2},8,8}$ is shown in Table 2. For this application it is convenient to have a numerical listing of all the indices in dictionary order with their $|E|$ and E^2-1 values, in order to look up the necessary $E^2_{\mathbf{h}+\mathbf{k}}-1$ terms. From the 10, 4, 4 term alone, the $P_+(E_{\bar{1}\bar{2},8,8})$ is 0·88. When the other $E_{2\mathbf{k}}$ with known signs were included in the summation, the $P_+(E_{\bar{1}\bar{2},8,8})$ rose to almost certainty.

Only those signs were accepted for which the corresponding probability was high. Of course, there were some $E_{2\mathbf{h}}$ for which Σ_3 was indeterminate. After quite a few + signs had been assigned, it was possible to get $-$ signs from Σ_3 with a high probability. An example is illustrated in Table 3.

Since E^2-1 cannot be greater than -1 in the negative direction, many negative terms are needed to get a large $P_-(E_{2\mathbf{h}})$. The one term alone in the example gave $P_-(E_{2\mathbf{h}})=0{\cdot}61$. It was found, however, that a great majority of the contributing terms gave an indication of a negative sign.

When about 15–25 signs had been found with Σ_3,

Table 1

2h	$E_{2\mathbf{h}}$	h	$E^2_{\mathbf{h}}-1$	$P_+(E_{2\mathbf{h}})$ (a)	$P_+(E_{2\mathbf{h}})$ (b)
$\bar{4}$ 4 10	3·19	$\bar{2}25$	+7·04	0·87	0·97
10 4 4	3·18	522	+10·61	0·94	~1·00
12 4 6	2·97	623	+9·00	0·90	~1·00
8 4 2	2·35	421	+6·93	0·80	0·84

Table 2

2h = $\bar{1}\bar{2}$ 8 8	($E_{2\mathbf{h}}=5{\cdot}67$)			
2k = 10 4 4	10 $\bar{4}$ 4	$\bar{1}\bar{0}$ $\bar{4}$ $\bar{4}$	$\bar{1}\bar{0}$ 4 $\bar{4}$	($E_{2\mathbf{k}}=+3{\cdot}18$)
h+k = $\bar{1}$ 6 6	$\bar{1}$ 2 6	$\bar{1}\bar{1}$ 2 2	$\bar{1}\bar{1}$ 6 2	
$E^2_{\mathbf{h}+\mathbf{k}}-1$ = +0·04	+3·45	−1·00	+13·35	

$$sE_{2\mathbf{h}} \sim +3{\cdot}18(+0{\cdot}04+3{\cdot}45-1{\cdot}00+13{\cdot}35)+\ldots$$

Table 3

2h = 0 8 2	($E_{2\mathbf{h}}=3{\cdot}00$)			
2k = $\bar{1}\bar{2}$ 8 8	$\bar{1}\bar{2}$ $\bar{8}$ 8	12 8 $\bar{8}$	12 $\bar{8}$ $\bar{8}$	($E_{2\mathbf{k}}=+5{\cdot}67$)
h+k = $\bar{6}$ 8 5	$\bar{6}$ 0 5	6 8 $\bar{3}$	6 0 $\bar{3}$	
$E^2_{\mathbf{h}+\mathbf{k}}-1$ = −0·79	−0·86	−0·92	−0·99	

$$sE_{2\mathbf{h}} \sim +5{\cdot}67(-0{\cdot}79-0{\cdot}86-0{\cdot}92-0{\cdot}99)+\ldots$$

they were reiterated in Σ_3 to check for internal consistency. At this point there were a sufficient number of known signs to use Σ_2,

$$sE_{\mathbf{h}} \sim s \sum_{\mathbf{k}} E_{\mathbf{k}} E_{\mathbf{h}+\mathbf{k}} . \qquad (3\cdot10)$$

In this formula, the signs of both $E_{\mathbf{k}}$ and $E_{\mathbf{h}+\mathbf{k}}$ need to be known in order to obtain the sign of $E_{\mathbf{h}}$. Again, only the terms with the largest E values were used to establish a basic set of signs. The signs determined by Σ_3 were confirmed by using Σ_2 whenever possible, e.g. the signs of $\bar{4}$, 4, 10 and 8, 4, 2 were assigned from Σ_1 and they combined to give the sign of $\bar{12}$, 8, 8:

$\bar{4}$ 4 10	$E_{\mathbf{k}} = +3\cdot19$
8 4 $\bar{2}$	$E_{\mathbf{h}+\mathbf{k}} = +2\cdot35$
$\bar{12}$ 8 8	$E_{\mathbf{h}} = 5\cdot67$

$$sE_{\bar{12},8,8} \sim (+3\cdot19)(+2\cdot35)$$

The probability that $E_{\bar{12},8,8}$ is + is 0·99 and is in agreement with the positive result from Σ_3. As many combinations of Σ_2 as possible should be used for every sign determined. For the $E_{\mathbf{h}}$ with the largest magnitudes, there should be extremely few, if any, inconsistent sign indications with Σ_2. As one proceeds to smaller magnitudes of $E_{\mathbf{h}}$, then some contradictions will occur and, at times, the sign may be indeterminate.

So far, the only signs determined have been in the group *ggg* (including 0*g*0 and *g*0*g*). It seems to be a good policy to determine the signs of only the largest E_{ggg} and then to proceed to the largest $E_{\mathbf{h}}$ in the other groups. Otherwise a false pattern of signs may be established which will be found to give large inconsistencies in the other groups. In order to begin in the other groups, it is necessary to arbitrarily assign three signs which fix the origin (Monograph I). Ordinarily, the largest $E_{\mathbf{h}}$ are chosen for the assigned signs. In this crystal, the *ugg* group had large E values, hence the largest, $E_{13,6,4} = 7\cdot17$, was made positive. The next largest *ugg* was $\bar{11}$, 6, 6 and Σ_2 with the known signs from the *ggg* group was used to determine its sign. There were two contributors:

$\bar{13}$ 6 4	(+7·17)		$\bar{13}$ $\bar{6}$ 4	(−7·17)
$\bar{2}$ 0 $\bar{2}$	(+3·69)	and	2 12 2	(−2·29)
$\bar{11}$ 6 6	6·53		$\bar{11}$ 6 6	6·53

$$sE_{\bar{11},6,6} \sim (+7\cdot17)(+3\cdot69)+(-7\cdot17)(-2\cdot29)$$

With the signs for $\bar{13}$, 6, 4 and $\bar{11}$, 6, 6, signs for many more E_{ugg} were determined with Σ_2. Arbitrary signs were also assigned to the largest *uug* and *ggu* reflections and others in these groups were determined with Σ_2. Finally, the signs in the four remaining groups were dependent upon the signs already obtained. For instance, in the *gug* group, combinations such as *ugg*+*uug*, *ggu*+*guu*, *ugu*+*uuu*, and *ggg*+*gug* were used in Σ_2.

Two hundred and seventy signs with $|E| > 2$ were assigned using Σ_1, Σ_2 and Σ_3. Some cross checking for consistency in groups other than *ggg* was performed using Σ_3. Since the sign determination was carried out by hand computing, it was not feasible to apply Σ_3 very extensively. Of the 270 phases, all but one subsequently proved to be correct.

In a set of 1732 Σ_2 combinations which were used to determine the signs, there were 116 contradictions to the correct sign. These contradictions did not usually interfere with the sign determination since there were several stronger terms indicating the correct sign. Table 4 lists the number of exceptions to Σ_2 and the corresponding $E_1E_2E_3/N^{\frac{1}{2}}$ product associated with

Table 4

$E_1E_2E_3/N^{\frac{1}{2}}$	Exceptions
5·0–11·0	0
4·0– 4·9	1
3·0– 3·9	9
2·0– 2·9	29
1·0– 1·9	77

them, where N is the number of atoms in the unit cell. The exceptions are related to $E_1E_2E_3/N^{\frac{1}{2}}$ since this quantity occurs in the probability expression for Σ_2 and since it is in a normalized form applicable to any crystal.

The largest exception had a value of 4·8 and it was the only exception out of 144 terms in the range 4·0–11·0. The exceptions followed an expected distribution in that the number was relatively small for large $E_1E_2E_3/N^{\frac{1}{2}}$ values and larger for smaller $E_1E_2E_3/N^{\frac{1}{2}}$ values.

4. Structure

The 270 reflections (6% of the non-zero data) for which signs had been determined were used to compute a three-dimensional E map. This is a Fourier in which the $E_{\mathbf{h}}$ rather than the $F_{\mathbf{h}}$ are used as coefficients. The E map was characterized by 37 main peaks, two of which were fairly weak. One of the weak peaks was spurious whereas the other 36 peaks were identified with the atoms of the two molecules in the asymmetric unit. The average weight of the six O atoms was 310, the average weight of the thirty C atoms was 266, and the rapidly oscillating background rarely reached ±100.

The coordinates of the atoms as read from the E map were subjected to a preliminary least-square refinement on the IBM 704, using the program prepared by D. Sayre. About 1100 structure-factor magnitudes sampled throughout the copper sphere of data (every fifth reflection ordered on $\sin\theta$) were used. One temperature factor per atom was used and the 28 hydrogen atoms in the asymmetric unit were omitted. At present, the R factor for the 1100 reflections used in the least-squares procedure, including all the zero reflections, is 22%*. The R factor for all 5527

* At this point it became apparent that the least-squares procedure was diverging owing to approximations in the program, and the computation was terminated.

Table 5. *Fractional atomic parameters*

	Molecule I				Molecule II		
Atom	*x/a*	*y/b*	*z/c*	Atom	*x/a*	*y/b*	*z/c*
O	0·432	0·680	0·077	O	0·434	0·686	0·585
O	0·225	0·370	0·220	O	0·227	0·376	0·731
O	0·435	0·064	0·067	O	0·424	0·069	0·543
C(CH_3)	0·429	0·751	0·185	C(CH_3)	0·381	0·763	0·578
C(CH_3)	0·387	0·985	0·062	C(CH_3)	0·419	0·995	0·629
C(CO)	0·292	0·372	0·174	C(CO)	0·294	0·378	0·678
C	0·398	0·607	0·112	C	0·396	0·612	0·612
C	0·361	0·595	0·225	C	0·311	0·608	0·611
C	0·327	0·515	0·239	C	0·282	0·526	0·631
C	0·329	0·451	0·149	C	0·328	0·457	0·651
C	0·366	0·467	0·040	C	0·412	0·466	0·650
C	0·404	0·545	0·013	C	0·446	0·544	0·625
C	0·327	0·289	0·135	C	0·330	0·296	0·649
C	0·278	0·219	0·116	C	0·327	0·228	0·730
C	0·311	0·140	0·091	C	0·357	0·153	0·708
C	0·394	0·137	0·099	C	0·391	0·145	0·594
C	0·445	0·204	0·107	C	0·397	0·210	0·498
C	0·410	0·282	0·137	C	0·367	0·286	0·531

reflections is 26%, and 22% if the reflections read to be zero are omitted. It would be worth while to refine the structure further both with three-dimensional Fouriers and with least squares, using anisotropic temperature factors and the complete set of data.

The present atomic coordinates are listed in Table 5. The two molecules in an asymmetric unit are illustrated in Fig. 1, a projection along the *a* axis, $\frac{1}{4} \leq x \leq \frac{1}{2}$.

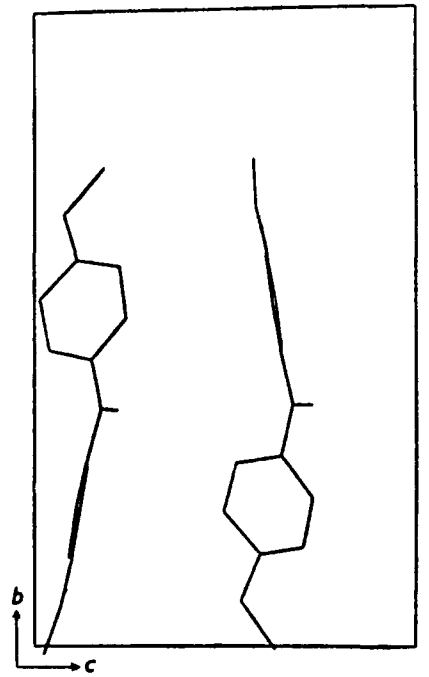

Fig. 1. Projection of an asymmetric unit along the *a* axis, $\frac{1}{4} \leq x \leq \frac{1}{2}$.

The three oxygen atoms in each molecule lie near the

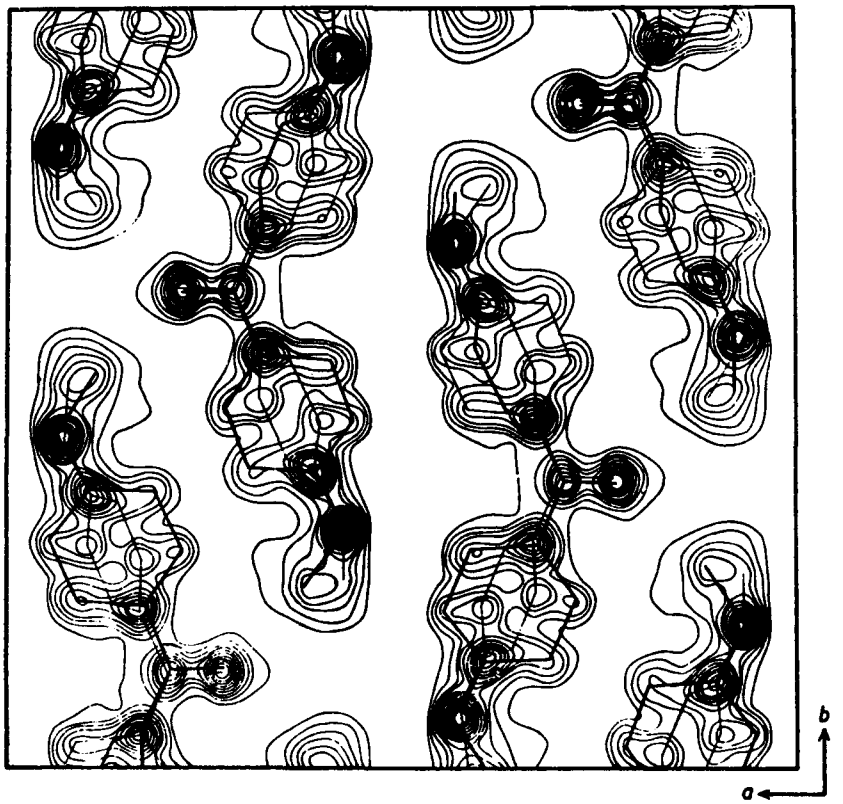

Fig. 2. Electron-density projection on (001). The pairs of superimposed molecules are separated by approximately $\frac{1}{2}c$. The coordinates of the line drawings were taken from the preliminary three-dimensional least-squares refinement.

202 planes. The molecules are related to each other approximately by a shift of $z+\frac{1}{2}$ and a reflection through $y=\frac{3}{8}$. The carbon atoms in the methoxy groups are very nearly in the same plane as the adjacent benzene rings. The top ring in molecule I and the bottom ring in molecule II are rotated about 38° out of the planes formed by the three oxygen atoms in each molecule, whereas the bottom ring in molecule I and the top ring in molecule II are rotated about 24° out of the plane of oxygen atoms.

Fig. 2 illustrates the contents of the unit cell as viewed down the c axis. The pairs of superimposed molecules are separated by approximately $\frac{1}{2}c$. The coordinates of the line drawings were taken from the least-squares refinement. The signs for the electron-density projection were derived from these coordinates where $R = 20\%$ for the z projection, including all terms. The same reflections and signs were used to compute the E map (E_{hk0} instead of F_{hk0} for the coefficients in the Fourier series) which is illustrated in Fig. 3. A comparison of the E map with the F map shows the much greater resolution of atoms in the superposed benzene rings and methyl groups in the E map. The contours near the centers of the atoms were not drawn owing to the fairly rough grid used in computing the series. The contours in the E map are on an arbitrary scale spaced by a value of 1, with the lowest contour at 2. The background oscillates very rapidly but does not exceed ±2.

The shortest intermolecular distances are between an oxygen and oxygen in methoxy groups at 3·41 Å and an oxygen and carbon at 3·45 Å. The average bonded distances with their average deviations at the present stage of refinement are listed in Table 6.

Table 6

Bond type	Average distance (Å)	Average deviation (Å)
C–C, ring	1·378	0·030
C–C, non-ring	1·475	0·030
C–O, aromatic	1·405	0·025
C–O, aliphatic	1·500	0·028
C=O	1·280	0·010

The C–O–C angles are 115° and the $C_{ar.}$–C–$C_{ar.}$ angle in the ketone group is 123°, which is the same as that found in p,p'-diiodobenzophenone (Manthey, Pleth & Singewald, 1952).

5. Theoretical basis for E maps

The value of removing the effect of the electron distribution and vibration in sharpening peaks in a Fourier series is well known. To our knowledge this sharpening has been applied mainly to the calculation of a Patterson series. It has been seen in this paper that it is worth while to compute sharpened Fourier series representing atomic positions using on the one hand only the largest E values as coefficients and on the other hand all E values contained within a particular sphere in reciprocal space. A Fourier series computed

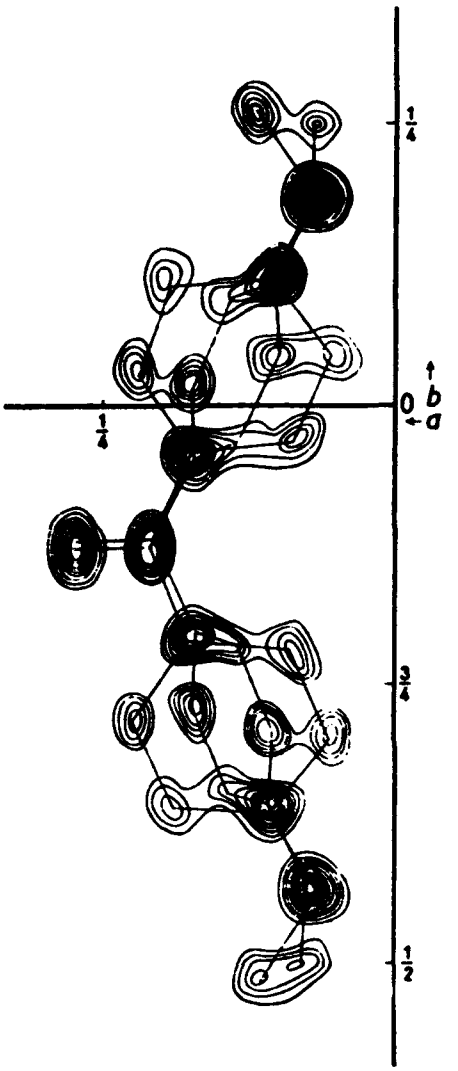

Fig. 3. An E map projection on (001). The same reflections and signs were used to compute the E map as those used in the F map, Fig. 2. The increased resolution over that in Fig. 2 is of interest.

from a restricted number of large E's is well adapted for use with direct methods of phase determination since the phases of the largest E's are the ones which are most easily determined. We present here the theoretical significance of such a calculation.

We define the structure factor

$$F_{\mathbf{h}_\mu} = X_{\mathbf{h}_\mu} + iY_{\mathbf{h}_\mu}, \tag{5·1}$$

where

$$X_{\mathbf{h}_\mu} = \sum_{j=1}^{N/n} f_{j\mathbf{h}_\mu}\xi_{j\mathbf{h}_\mu}, \tag{5·2}$$

$$Y_{\mathbf{h}_\mu} = \sum_{j=1}^{N/n} f_{j\mathbf{h}_\mu}\eta_{j\mathbf{h}_\mu}, \tag{5·3}$$

N is the number of atoms in the unit cell, n is the symmetry number, $f_{j\mathbf{h}_\mu}$ is the atomic scattering factor, and the values of the real and imaginary parts $X_{\mathbf{h}_\mu}$ and $Y_{\mathbf{h}_\mu}$ of the structure factor $F_{\mathbf{h}_\mu}$ are known to be

$A_{\mathbf{h}\mu}$ and $B_{\mathbf{h}\mu}$ respectively. The ξ and η are the trigonometric functions of the atomic coordinates listed in *International Tables* (1952) for the various space groups. It was shown (Karle & Hauptman, 1954) that the most probable values of the coordinates x_k, y_k, z_k of those atoms characterized by the atom scattering factor f_k coincide (to good approximation) with the principal maxima of

$$\exp\left\{\sum_{\mu=1}^{m} \frac{-(A_{\mathbf{h}\mu}-f_{k\mathbf{h}\mu}\xi_{k\mathbf{h}\mu})^2-(B_{\mathbf{h}\mu}-f_{k\mathbf{h}\mu}\eta_{k\mathbf{h}\mu})^2}{2m_2\sum_{j=2}^{N/n} f_{j\mathbf{h}\mu}^2}\right\}, \quad (5\cdot4)$$

where, subject to $m_2 \neq 0$,

$$m_2 = m_2^0 = \int_0^1\int_0^1\int_0^1 \xi_{j\mathbf{h}\mu}^2\,dx_j dy_j dz_j$$

or

$$m_2 = m_0^2 = \int_0^1\int_0^1\int_0^1 \eta_{j\mathbf{h}\mu}^2\,dx_j dy_j dz_j\,. \quad (5\cdot5)$$

In the cases that either m_2^0 or m_0^2 equals zero, m_2 equals the non-zero moment. If we take the logarithm of (5·4) and expand the squares, we obtain

$$\sum_{\mu=1}^{m} \frac{1}{2m_2\sum_{j=2}^{N/n} f_{j\mathbf{h}\mu}^2}(-A_{\mathbf{h}\mu}^2-B_{\mathbf{h}\mu}^2+2f_{k\mathbf{h}\mu}(A_{\mathbf{h}\mu}\xi_{k\mathbf{h}\mu}+B_{\mathbf{h}\mu}\eta_{k\mathbf{h}\mu}) - f_{k\mathbf{h}\mu}^2(\xi_{k\mathbf{h}\mu}^2+\eta_{k\mathbf{h}\mu}^2))\,. \quad (5\cdot6)$$

As pointed out by Bullough & Cruickshank (1954), the main term in (5·6) is

$$\sum_{\mu=1}^{m} \frac{f_{k\mathbf{h}\mu}}{m_2\sum_{j=2}^{N/n} f_{j\mathbf{h}\mu}^2}(A_{\mathbf{h}\mu}\xi_{k\mathbf{h}\mu}+B_{\mathbf{h}\mu}\eta_{k\mathbf{h}\mu})\,. \quad (5\cdot7)$$

the first two terms of (5·6) being a numerical constant and the last is space-group, though not structure, dependent, and is also not expected to have an important effect upon the maxima. The last term is seen to be a numerical constant for space group $P1$.

Expression (5·7) is a Fourier series and we are interested in seeing how the coefficients of the real and imaginary parts are related to the normalized structure factor $E_{\mathbf{h}\mu}$, defined by

$$E_{\mathbf{h}\mu} = \frac{F_{\mathbf{h}\mu}}{((m_2^0+m_0^2)\sum_{j=1}^{N/n} f_{j\mathbf{h}\mu}^2)^{\frac{1}{2}}} = \frac{X_{\mathbf{h}\mu}+iY_{\mathbf{h}\mu}}{((m_2^0+m_0^2)\sum_{j=1}^{N/n} f_{j\mathbf{h}\mu}^2)^{\frac{1}{2}}}\,. \quad (5\cdot8)$$

If we ignore numerical constants, we have for the coefficients of the first and second terms in (5·7), respectively

$$\frac{f_{k\mathbf{h}\mu}}{\left(\sum_{j=2}^{N/n} f_{j\mathbf{h}\mu}^2\right)^{\frac{1}{2}}}\cdot\frac{A_{\mathbf{h}\mu}}{\left(\sum_{j=2}^{N/n} f_{j\mathbf{h}\mu}^2\right)^{\frac{1}{2}}}\,, \quad (5\cdot9)$$

and

$$\frac{f_{k\mathbf{h}\mu}}{\left(\sum_{j=2}^{N/n} f_{j\mathbf{h}\mu}^2\right)^{\frac{1}{2}}}\cdot\frac{B_{\mathbf{h}\mu}}{\left(\sum_{j=2}^{N/n} f_{j\mathbf{h}\mu}^2\right)^{\frac{1}{2}}}\,. \quad (5\cdot10)$$

The first term in the product (5·9) is the same as the first term of (5·10). It is essentially a constant and if all atoms are assumed to have the same shape, it is an exact constant. Now consider the second terms in (5·9) and (5·10). The numerators are the known values of the real and imaginary parts of the structure factor and the sum in the denominators differs from the sum in (5·8) by a single term. We may conclude that the coefficients in (5·7) are proportional to $E_{\mathbf{h}\mu}$ and we are thus led to the significance of an E map, namely: The maxima of an E map answer the following question: 'What are the most probable values of the atomic coordinates given the values of any set of structure factors?'.

We wish to thank many people for their invaluable assistance. Mr C. E. Miller of Bell Telephone Laboratories prepared the crystals; Dr S. Geller of the same laboratory obtained preliminary crystallographic data and suggested that the probability method be applied to this crystal; Mr P. O'Hara of the National Bureau of Standards, Dr H. T. Evans of the Geological Survey, and Mr R. A. Sparks of the University of California in Los Angeles performed the various calculations for the K curve, the E maps and the electron-density projection; and Mr A. Hatch of the Service Bureau Corporation applied the least-squares program developed by Dr D. Sayre.

References

Bertaut, E. F. (1955). *Acta Cryst.* **8**, 823.

Bertaut, E. F. & Blum, P. (1956). *Acta Cryst.* **9**, 121.

Bullough, R. K. & Cruickshank, D. W. J. (1954). *Acta Cryst.* **7**, 598.

Christ, C. L. & Clark, J. R. (1956). *Acta Cryst.* **9**, 830.

Christ, C. L., Clark, J. R. & Evans, H. T. Jr. (1954). *Acta Cryst.* **7**, 453.

Hauptman, H. & Karle, J. (1953). *Solution of the Phase Problem. I. The Centrosymmetric Crystal.* A.C.A. Monograph No. 3. Brooklyn: Polycrystal Book Service.

Hauptman, H. & Karle, J. (1957). *Acta Cryst.* **10**, 267.

Hauptman, H. & Karle, J. (1958). *Acta Cryst.* **11**, 149.

International Tables for X-ray Crystallography (1952). Birmingham: Kynoch Press.

Karle, J. & Hauptman, H. (1953). *Acta Cryst.* **6**, 473.

Karle, J. & Hauptman, H. (1954). *Acta Cryst.* **7**, 375.

Karle, J. & Hauptman, H. (1957). *Acta Cryst.* **10**, 515.

Karle, J. & Hauptman, H. (1958). *Acta Cryst.* **11**, 264.

Karle, I. L., Hauptman, H., Karle, J. & Wing, A. B. (1957). *Acta Cryst.* **10**, 481.

Manthey, W., Plieth, K. & Singewald, A. (1952). *Z. Elektrochem.* **56**, 690.

Vand, V. & Pepinsky, R. (1953). *The Statistical Approach to X-ray Structure Analysis.* Pennsylvania State University: X-ray and Crystal Analysis Laboratory.

Wilson, A. J. C. (1949). *Acta Cryst.* **2**, 318.

Wing, A. B. & Birks, L. S. (1954). Naval Research Laboratory Report 4402.

Woolfson, M. M. (1954). *Acta Cryst.* **7**, 61.

Profiles in Science

The whole of science is nothing more than a refinement of everyday thinking.

Albert Einstein (1936)

Theodor Wieland

Theodor Wieland is Professor Emeritus and formerly Director of the Chemistry Department of the Max-Planck-Institute, Heidelberg. He retired in 1981. Professor Wieland's PhD thesis on toad poisons was done under the tutelage of his father, Professor Heinrich Wieland of the Chemical Institute, the University of Munich. While at the University of Heidelberg in 1937, Wieland pursued vitamin research and succeeded in isolating pantothenic acid from fish liver; he studied their biosynthesis and the separation of animo acids by chromatography and paper electrophoresis. After World War II, he was an associate professor at the University of Mainz working mainly on peptide syntheses (mixed anhydride method, active amino acid thiol esters) and poisons from Amanita mushrooms. In 1951, he became Director of the Institute of Organic Chemistry at the University of Frankfurt and completed the structural and analytical chemistry of the amatoxins and the phallotoxins and isolated the antitoxin cyclodecapeptide antamanide. It was this compound which brought him to Isabella Karle in 1973 when she agreed to investigate its structure.

Dr. Bernhard Witkop

Dr. Bernhard Witkop retired from the National Institute of Health in 1993 after a distinguished tenure of 42 years. Since 1956 he was chief of the section on metabolites in the Laboratory of Chemistry of the National Institute of Arthritis and Metabolic Diseases. He is well known for developing the cyanogen bromide reaction, a method for cleaving proteins precisely in order to facilitate the sequencing of a protein. The technique was a key development in the current genetic engineering revolution since protein sequencing is needed before a gene can be properly cloned. Witkop and his coworkers have helped define the metabolic pathways of many biologically important molecules, including serotonin, a neurotransmitter, and its precursor tryptophan, which is important for normal growth. For more than 30 years Bernhard Witkop and Isabella Karle have collaborated on research projects. Most noteworthy are: (1) the structure of the venom of the Colombian arrow poison frog, batrachotoxin(in), at the time probably the record for establishing a complete structure with an incredibly small crystal; and (2) the photolysis of n-chloroacetyl-o-methyl-l-tyrosine to an azulene is probably the first application of X-ray diffraction to such a complicated molecule of completely unknown chemical structure.

Dr. Arnold Brossi

Dr. Arnold Brossi is a visiting research professor of chemistry at Georgetown University, Washington, D.C. From 1976 to 1991, he was Chief of the Section of Natural Product Chemistry at the National Institute of Diabetes and Digestive Kedney Diseases, at the National Institute of Health. His major research interests include study and synthesis of biologically active natural products and drugs useful in malaria chemotherapy. He has specialized in studies of antipodal isomers. His work, spanning five decades has had a great impact on medical research and has led to the discovery of several drugs (Tetrabenazine, Dehydroemetine, Dimecaptosuccinic Acid, Astiban, Versidyne, Arteether and Phenserines). Besides using routine spectroscopic data for characterizing compounds, Brossi had early access to X-ray crystallography at the Naval Research Laboratory. Working with Isabella Karle and J.L. Flippen-Anderson, he used X-ray analysis to determine the absolute configuration of optically active compounds for elucidating the three-dimensional configuration of complex molecules and conformations of bioactive molecules.

Reprinted from *Acta Crystallographica*, Vol. 17, Part 7, July 1964

PRINTED IN DENMARK

Acta Cryst. (1964). **17**, 835

An Application of the Symbolic Addition Method to the Structure of L-Arginine Dihydrate

BY ISABELLA L. KARLE AND J. KARLE

U.S. Naval Research Laboratory, Washington 25, D.C., U.S.A.

(*Received 25 July 1963*)

The crystal structure of L-arginine dihydrate was determined directly by means of the symbolic addition phase determination procedure, using the complete three-dimensional data obtained from Cu radiation. The space group is $P2_12_12_1$ and the cell dimensions are:

$$a = 5{\cdot}68,\ b = 11{\cdot}87,\ \text{and}\ c = 15{\cdot}74\ \text{Å}.$$

The arginine molecule is a zwitterion with the guanidyl group, rather than the amino group, accepting an extra proton. Two planes characterize the arginine molecule, one through the acid group, and the other through the extended side chain which contains the guanidyl group. The dihedral angle between these planes is 74°. The arginine molecules and the water molecules each make infinite chains perpendicular to each other by hydrogen bonding. All 18 hydrogen atoms have been located.

Introduction

L-Arginine, $^{+}(H_2N)_2CNH(CH_2)_3CH(NH_2)COO^{-}$, is one of the amino acids essential for animal growth. It is also the most basic of the amino acids since, in addition to the α-amino group, it also contains a terminal guanidyl group. This investigation afforded a good opportunity to study a biologically important amino acid structure and its associated hydrogen bonding. It also provided a valuable experience in the first application of the symbolic addition method for phase determination (Karle & Karle, to be published) to a non-centrosymmetric crystal.

Experimental

Purified L-arginine was obtained from the Central Research Laboratories of General Mills, Inc. Recrystallization from water at room temperature yielded crystals of the dihydrate which were colorless, transpa-

rent prisms. They were elongated along the a axis. Crystals kept in air lost their sharp edges and appeared to deliquesce, whereas those kept in a desiccator became opaque and cracked. The crystals kept in the X-ray beam however were fairly well preserved. Eventually they showed signs of disintegration in the region where the X-ray beam impinged upon them.

Complete intensity data for Cu $K\alpha$ radiation were collected along the a, b and c axes by the multiple-film equi-inclination Weissenberg technique. Precession photographs for the $0kl$, $h0l$ and $hk0$ layers were also taken. No correction for absorption was made.

The space group is $P2_12_12_1$ and the unit cell parameters are:

$a = 5{\cdot}68 \pm 0{\cdot}01$, $b = 11{\cdot}87 \pm 0{\cdot}02$, $c = 15{\cdot}74 \pm 0{\cdot}02$ Å.

The computed density is $1{\cdot}314$ g.cm^{-3} and the measured density by flotation in mixed solvents was found to be $1{\cdot}320$ g.cm^{-3}.

Phase determination

The normalized structure factor $E_{\mathbf{h}}$ is defined by

$$E_{\mathbf{h}}^2 = F_{\mathbf{h}}^2/\varepsilon \sum_{j=1}^{N} f_{j\mathbf{h}}^2 \qquad (1)$$

where $\varepsilon = 2$ when $\mathbf{h}$ is $h00$, $0k0$ or 001, $\varepsilon = 1$ otherwise for space group $P2_12_12_1$, and f_j is the atomic scattering factor for the jth atom in the unit cell containing N atoms. Phases corresponding to 400 of the largest $|E_{\mathbf{h}}|$ were determined by means of the symbolic addition procedure for non-centrosymmetric space groups. The procedure is an extension of the symbolic addition method applied to centrosymmetric crystals (Karle & Karle, 1963; Karle, Britts & Gum, 1964).

The formula for starting the phase determination is (Karle & Karle, to be published),

$$\varphi_{\mathbf{h}} \approx \langle \varphi_{\mathbf{k}} + \varphi_{\mathbf{h}-\mathbf{k}} \rangle_{\mathbf{k}_r}, \qquad (2)$$

where the $\varphi_{\mathbf{h}}$ are the phases associated with the $|E_{\mathbf{h}}|$ and $\mathbf{k}_r$ implies that the average is taken only over those $\mathbf{k}$ corresponding to the larger $|E|$ values. Formula (2) is implemented by specifying appropriate phases (Hauptman & Karle, 1956) in order to fix the origin, and by assigning additional symbols to represent the phases associated with certain appropriately chosen reflections.

In space group $P2_12_12_1$, it is convenient to fix the origin by assigning the phases of two-dimensional data. The phases were assigned as follows:

h	$\varphi_{\mathbf{h}}$	$\|E_{\mathbf{h}}\|$
3,0,10	0	3·46
3,3, 0	$-\pi/2$	2·17
3,0, 1	$+\pi/2$	2·77

With these assignments, it is immediately possible to obtain contributors to (2) for particular $\varphi_{\mathbf{h}}$. For example, the largest guu is $|E_{631}| = 2{\cdot}06$. We note that if $\mathbf{k} = 301$ and $\mathbf{h}-\mathbf{k} = 330$, $\mathbf{h} = 631$. Since $\varphi_{330} = -\pi/2$ and $\varphi_{301} = +\pi/2$, this pair contributes the value zero toward the average in (2) for φ_{631}. Similarly, since $\varphi_{\bar{3},0,10} = \pi$ and the value zero may be used for φ_{631} at this stage, this pair contributes the value of π to the average in (2) for $\varphi_{3,3,11}$. $|E_{3,3,11}| = 2{\cdot}05$, the second largest uuu. Two pairs of contributors are now available for $\varphi_{0\bar{3}10}$ ($|E_{0\bar{3}10}| = 1{\cdot}85$) as follows:

h	$\varphi_{\mathbf{h}}$	h	$\varphi_{\mathbf{h}}$
$\bar{3}$,0, $\bar{1}$	$-\pi/2$	3,3, 0	$-\pi/2$
3,3,11	π	$\bar{3}$,0,10	π
0,3,10	$+\pi/2$	0,3,10	$+\pi/2$

Further contributors to new phases and also to φ_{631}, φ_{3311} and $\varphi_{0\bar{3}10}$ were developed by continuing the process of forming pairs as required by (2). In order to facilitate this, it was necessary to assign symbols to other phases. The assignments were,

h	$\varphi_{\mathbf{h}}$	$\|E_{\mathbf{h}}\|$
2,12, 0	p	3·21
2,10, 0	s	2·31
4, 0,14	m	2·56
3, 8, 3	a	2·31

These reflections were chosen because they entered into many of the combinations for the average in (2) and they were associated with relatively large $|E|$ values.* The symbols p, s, m must be either 0 or π, but a can be anywhere in the range $-\pi < a \leq \pi$. In forming the contributors to (2), maximum use was made of the three-dimensional reflections ($hkl \neq 0$). Too much reliance on two-dimensional reflections may lead to misleading phase indications.

In the course of application of the procedure, it soon became apparent that $m = \pi$. It was also apparent that a was near 0 or π. It was chosen to be zero, which, in effect, specified the enantiomorph. The specification of the enantiomorph for space group $P2_12_12_1$ is discussed in detail by Karle & Hauptman (1956).

By means of hand computation, 137 phases were determined in terms of $0, \pi, \pm\pi/2, p$, and s. Relatively few inconsistencies were found for pairs involving three-dimensional reflections or a three-dimensional and a two-dimensional reflection. However, there were a number of inconsistencies for pairs composed solely of two-dimensional data.

Since p and s have to be 0 or π, most phases in this first approximation were on the cardinal points, $0, \pi$ or $\pm\pi/2$. Some, however, were found to have intermediate values. For example, an approximately equal number of contributors to (2) might consist of the types $-\pi/2+s$ and $p+s$. The average, $\frac{1}{2}[(-\pi/2+s)+(p+s)]$, would then have the possible values, $\pi/4$, $-\pi/4$, $3\pi/4$ or $-3\pi/4$, depending upon the values of p and s.

* A procedure based on the multiplication of symbols, rather than addition, can be used if the symbols represent $\exp(i\varphi)$ rather than φ.

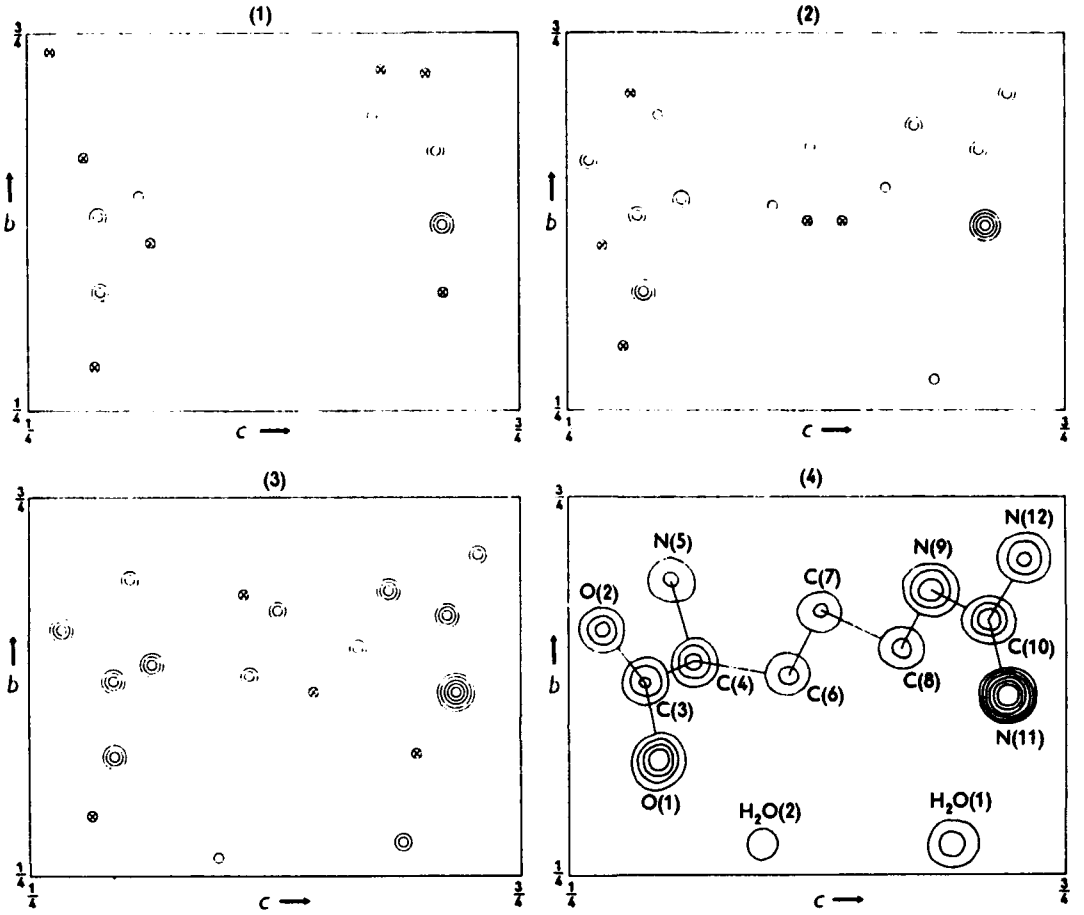

Fig. 1. Three-dimensional E-maps for arginine, viewed along the a axis, which were computed with normalized structure factors, E, as coefficients. The phases were obtained from the symbolic addition procedure. (1) 137 data with $|E|_{\min}=1{\cdot}50$, (2) 200 data with $|E|_{\min}=1{\cdot}40$, (3) 300 data with $|E|_{\min}=1{\cdot}15$, and (4) 400 data with $|E|_{\min}=1{\cdot}00$. The peaks marked with crosses are extraneous. The contours are at equal intervals on an arbitrary scale.

The following four combinations of values for p and s,

p	s
0	π
π	0
0	0
π	π

were substituted into the set of 137 phases defined in terms of these symbols. Each of the four sets of phases so obtained was used as a basic set for the application of the tangent formula (Karle & Hauptman, 1956)

$$\tan \varphi_{\mathbf{h}} \approx \frac{\sum_{\mathbf{k}_r} |E_{\mathbf{k}} E_{\mathbf{h}-\mathbf{k}}| \sin(\varphi_{\mathbf{k}}+\varphi_{\mathbf{h}-\mathbf{k}})}{\sum_{\mathbf{k}_r} |E_{\mathbf{k}} E_{\mathbf{h}-\mathbf{k}}| \cos(\varphi_{\mathbf{k}}+\varphi_{\mathbf{h}-\mathbf{k}})}, \qquad (3)$$

where $\mathbf{k}_r$ ranges over 137 values of $\mathbf{k}$. This formula is used to reiterate the determination of values for the initial set of phases and to obtain additional ones. Since the numerator of (3) is proportional to $|E_{\mathbf{h}}|\sin\varphi_{\mathbf{h}}$ and the denominator of (3) is proportional to $|E_{\mathbf{h}}|\cos\varphi_{\mathbf{h}}$, the sum of the squares would be proportional to $|E_{\mathbf{h}}|^2$. If this formula is calculated for many $\mathbf{h}$ values, the proportionality constant may be obtained from a comparison with the experimental values for $|E_{\mathbf{h}}|^2_{\text{obs}}$ over the same range of $\mathbf{h}$. The adjustment is made by setting the average of the calculated $|E_{\mathbf{h}}|^2_{\text{calc}}$ equal to the average of the observed $|E_{\mathbf{h}}|^2_{\text{obs}}$. In the course of the calculation those reflections were eliminated whose $|E_{\mathbf{h}}|_{\text{calc}}$ were very small. An arbitrary level of 0·3 was chosen. Reflections whose phases changed greatly from reiteration cycle to reiteration cycle were also eliminated. Usually, the tangent formula (3) converges in one or two iterations if no new data are introduced.

The correct answer was found to correspond to the combination $p=s=\pi$. The other three combinations did not produce E-maps which were crystallographically meaningful. E-maps are Fourier maps employing the $E_{\mathbf{h}}$ as coefficients (Karle, Hauptman, Karle & Wing, 1958). Fig. 1 shows E-maps calculated for (1) 137 data (minimum $|E|=1{\cdot}50$), (2) 200 data (minimum $|E|=1{\cdot}40$), (3) 300 data (minimum $|E|=1{\cdot}15$), (4) 400 data (minimum $|E|=1{\cdot}00$). It is seen that

calculation (3) of Fig. 1 reveals the molecular structure quite well. This map includes about one fifth of the total data collected. The peaks marked with crosses are extraneous. In calculation (4) of Fig. 1, there were no extraneous peaks as strong as the fourteen peaks which corresponded to the structure.

It is of interest to note that phase-determining formulas obtained in the past, which define phases in terms of structure factor magnitudes, could have been used to determine the correct values of p and s directly. One type of formula which could have been used is the Σ_1 formula for space group $P2_12_12_1$ (Karle & Hauptman, 1956). The two forms of interest are

$$SE_{2h,2k,0} \sim S\sum_l (-1)^{l+k}(|E_{hkl}|^2-1), \qquad (4)$$

and

$$SE_{0,2k,2l} \sim S\sum_h (-1)^{h+k}(|E_{hkl}|^2-1), \qquad (5)$$

where S means 'sign of'. Table 1 shows the results of the application of (4) and (5). There were nineteen terms in the sum for (4) and seven in the sum for (5). The probability that the sign be positive for the E_{2h} in question, $P_+(E_{2h})$, is given by

$$P_+(E_{2h}) = \tfrac{1}{2} + \tfrac{1}{2}\tanh \sigma_3|E_{2h}|\Sigma_1/2\sigma_2^{3/2} \qquad (6)$$

where Σ_1 is the sum contained in (4) or (5), and $\sigma_n = \sum_{j=1}^{N} Z_j^n$, Z_j being the atomic number of the jth atom in a unit cell containing N Atoms. It is seen from Table 1 that three determinations indicate that p has a value of π with probabilities 0·86, 0·72, and 0·73, and s has a value of π with probabilities 0·85 and 0·72. The over-all probability from the three determinations that p is equal to π is about 0·97 and that for s from the two determinations is about 0·94, assuming that the determinations are independent.

Table 1. *An application of the Σ_1 formula*

2h	symbol	Σ_1	$P_+(E_{2h})$
2,12, 0	p	−	0·14
2,10, 0	s	−	0·15
4, 8, 0	$\pi+p$	+	0·72
0,12, 8	p	−	0·27
0,10,14	s	−	0·28

Another type of phase-determining formula which could have been used for determining the value of p and s is $B_{3,0}$ (Karle & Hauptman, 1958). With this formula there were several indications that the values of p and s were π. The value of m was also found to be π. It is interesting to note that when the data were extended by use of a Patterson map, improved by the application of a positivity criterion (Karle & Hauptman, 1964), the results of formula $B_{3,0}$ were more definitive.

In the initial set of 137 phases obtained from formula (2), the phases of the three-dimensional reflections had errors which were distributed as indicated by the dashed curve in Fig. 2. The symbol φ_{error} is defined as the magnitude of the difference between a phase calculated for the refined structure and one calculated from (2) or (3). It is seen from the solid curve that application of (3) to the initial phases improved their values considerably. The average error for the three-dimensional phases decreased from 43° to 27° by the use of the tangent formula.

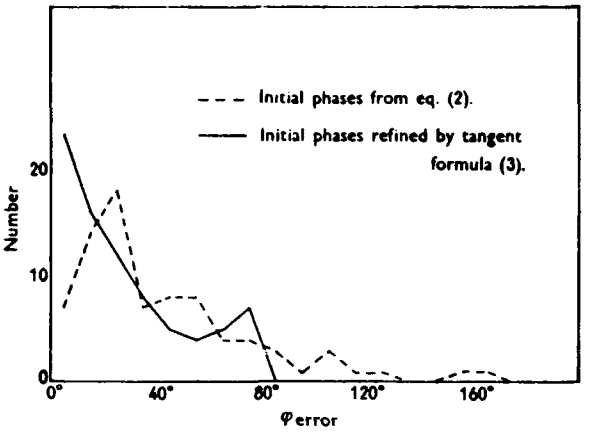

Fig. 2. The magnitude of the difference between the initial values of phases for three-dimensional reflections and the final values calculated from the refined structure.

Refinement

The preliminary coordinates of the fourteen atoms, other than hydrogen, which were obtained from the fourth E-map in Fig. 1, were subjected to a three-dimensional least-squares refinement (Busing, Martin & Levy, 1962) using all the 1406 data. After two cycles, employing isotropic temperature factors, the R index was 14·8%. Next, two cycles with anisotropic temperature factors reduced the R index to 11·6%. All the terms were evenly weighted with the value of one. At this point, a difference Fourier synthesis was computed in order to find the hydrogen atoms. All 18 hydrogen atoms were located. One more refinement was performed which included all the 32 atoms. Then another difference map was computed, which used the ΔF from the heavier atoms alone while the phase angles included the calculated contributions from the hydrogen atoms as well. The final R index was 10·3%.*

The difference map showing the location of the 18 hydrogen atoms is illustrated in Fig. 3. It is a composite drawing projected along the a axis. Although the coordinates of the hydrogen atoms have not been extensively refined, there is no doubt about the approximate location of each hydrogen and the configuration about the heavy atom to which it is bonded. A final electron density map computed with F values

* A microfilm containing the observed F and the computed F, A and B has been deposited with the Library of Congress, Washington, D.C., U.S.A. The reel number is 8496.

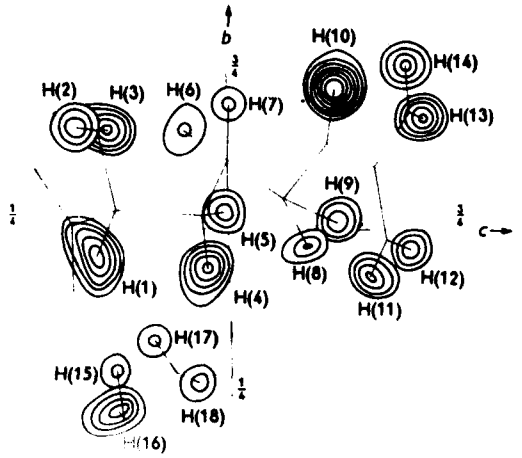

Fig. 3. A projection along the a axis of sections of a difference map for the location of hydrogen atoms. Contours are at intervals of 0·05 e.Å^{-3}, starting with the 0·15 e.Å^{-3} contour.

Table 3. *The approximate coordinates for the hydrogen atoms as determined from the second difference map*

Atom	Bonded to	x	y	z
H(1)	C(4)	0·908	0·458	0·350
H(2)	N(5)	0·847	0·650	0·328
H(3)	N(5)	0·938	0·645	0·362
H(4)	C(6)	0·076	0·442	0·475
H(5)	C(6)	0·933	0·525	0·495
H(6)	C(7)	0·366	0·645	0·450
H(7)	C(7)	0·208	0·682	0·502
H(8)	C(8)	0·388	0·478	0·589
H(9)	C(8)	0·253	0·512	0·623
H(10)	N(9)	0·525	0·703	0·617
H(11)	N(11)	0·722	0·433	0·660
H(12)	N(11)	0·862	0·472	0·705
H(13)	N(12)	0·933	0·663	0·719
H(14)	N(12)	0·822	0·741	0·700
H(15)	W(1)	0·533	0·207	0·629
H(16)	W(1)	0·459	0·267	0·628
H(17)	W(2)	0·558	0·335	0·412
H(18)	W(2)	0·558	0·275	0·463

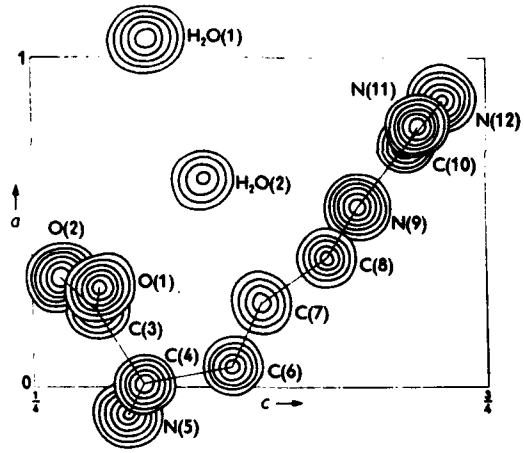

Fig. 4. A projection along the b axis of sections of the final electron density map. Only one arginine molecule is shown. Contours are at intervals of 1 e.Å^{-3}, starting with the 1·5 e.Å^3 contour.

is shown in Fig. 4. This composite drawing is viewed along the b axis.

The final coordinates and anisotropic temperature factors for the heavier atoms are listed in Table 2. The approximate coordinates for the hydrogen atoms are given in Table 3.

Geometry of the molecule

The arginine molecule is characterized by two planes, one through the carboxyl group and the other through the side chain which terminates with the guanidyl group. The molecule is a zwitterion with the guanidyl group, rather than the amino group, accepting a proton from the acid group. The bond lengths and angles are listed in Table 4 and shown in Fig. 5.

The dimensions of the amino acid group are quite similar to those reported for glycine (Marsh, 1958) and L-lysine (Wright & Marsh, 1962). The equation

Table 2. *The final parameters and their standard deviations*

The thermal parameters are of the form $T=\exp[-(\beta_{11}h^2+\beta_{22}k^2+\beta_{33}l^2+2\beta_{12}hk+2\beta_{13}hl+2\beta_{23}kl)]$. For the oxygen atoms of the water molecules, the alternate symbols W(1) and W(2) are used in the succeeding Tables. The standard deviations are multiplied by 10^4

	x	σ_x	y	σ_y	z	σ_z	$10^4\beta_{11}$	$10^4\beta_{22}$	$10^4\beta_{33}$	$10^4\beta_{12}$	$10^4\beta_{13}$	$10^4\beta_{23}$
O(1)	0·3022	(11)	0·4036	(4)	0·3231	(4)	244	44	42	23	68	4
O(2)	0·3340	(11)	0·5832	(4)	0·2830	(4)	219	45	31	6	53	2
C(3)	0·2353	(14)	0·5047	(6)	0·3220	(4)	162	41	17	−2	16	3
C(4)	0·0072	(11)	0·5293	(5)	0·3724	(4)	95	35	14	−4	6	−3
N(5)	−0·0839	(11)	0·6432	(6)	0·3524	(4)	136	44	23	7	0	−2
C(6)	0·0622	(13)	0·5186	(7)	0·4680	(4)	149	56	12	−31	1	1
C(7)	0·2546	(17)	0·5995	(7)	0·5002	(5)	288	59	19	−45	−52	11
C(8)	0·3822	(14)	0·5478	(7)	0·5753	(5)	148	52	22	−14	−39	11
N(9)	0·5532	(11)	0·6274	(5)	0·6118	(3)	127	37	14	−3	−24	1
C(10)	0·7315	(12)	0·5955	(6)	0·6633	(4)	110	46	10	−12	8	−2
N(11)	0·7796	(12)	0·4862	(5)	0·6760	(4)	161	36	16	9	−6	6
N(12)	0·8579	(13)	0·6739	(6)	0·7016	(4)	191	41	24	−1	−52	1
H$_2$O(1), W(1)	0·5506	(13)	0·2790	(6)	0·6214	(5)	252	45	66	17	25	6
H$_2$O(2), W(2)	0·6222	(17)	0·2871	(12)	0·4356	(5)	323	195	50	89	42	28

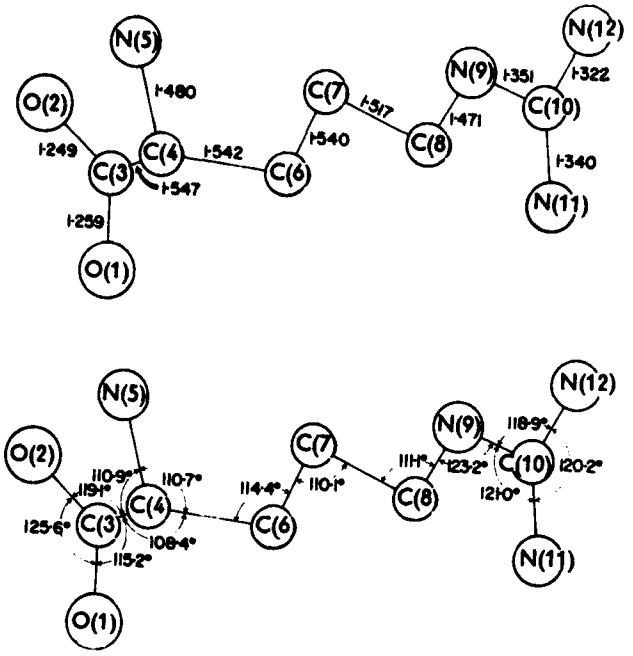

Fig. 5. Bond distances and angles.

for the least-squares plane through the atoms O(1)O(2)C(3)C(4) is

$$3{\cdot}1187x + 2{\cdot}3040y + 12{\cdot}795z = 6{\cdot}0093 \qquad (7)$$

and the deviations of the individual atoms from the plane are:

O(1) −0·003, O(2) −0·003, C(3) +0·008, and C(4) −0·002 Å.

Table 4. *Bond lengths and angles*

Bond		Angle	
C(3)–O(1)	1·259 Å	O(1)–C(3)–O(2)	125·6°
C(3)–O(2)	1·249	O(1)–C(3)–C(4)	115·2
		O(2)–C(3)–C(4)	119·1
C(4)–N(5)	1·480	C(3)–C(4)–N(5)	110·9
		C(6)–C(4)–N(5)	110·7
C(8)–N(9)	1·471	C(8)–N(9)–C(10)	123·2
C(10)–N(9)	1·351	N(9)–C(10)–N(11)	121·0
C(10–N(11)	1·340	N(9)–C(10)–N(12)	118·9
C(10)–N(12)	1·322	N(11)–C(10)–N(12)	120·2
C(3)–C(4)	1·547	C(3)–C(4)–C(6)	108·4
C(4)–C(6)	1·542	C(4)–C(6)–C(7)	114·4
C(6)–C(7)	1·540	C(6)–C(7)–C(8)	110·1
C(7)–C(8)	1·517	C(7)–C(8)–N(9)	111·1

The standard deviation for the bond lengths is 0·008 to 0·012 Å and for the angles 0·9°.

The nitrogen atom N(5) lies 0·280 Å out of the plane; the values found in glycine and lysine were near 0·44 Å. Although the amino group does not accept an extra proton to form C–NH_3^+ as was the case, for example, in glycine and lysine, the nitrogen in the amino group does assume a tetrahedral configuration with C(4), H(2) and H(3), and the fourth position on N(5) is occupied by a hydrogen bond from N(9′).

The guanidyl group is attached to the carbon chain by a C–N bond of 1·471 Å, whereas the three C–N bonds in the guanidyl group are nearly equal and average 1·338 Å. The C–N bonds in urea were found to be 1·336 Å (see, *e.g.* Sklar, Senko, & Post, 1961), 1·34 Å in nitroguanidine (Bryden, Burkardt, Hughes & Donohue, 1956), and 1·34 Å in guanidinium bromate (Drenth, Drenth, Vos & Wiebenga, 1953). The N–C–N angles are nearly 120° and the guanidyl group is planar. The equation of the least-squares plane through the atoms N(9)C(10)N(11)N(12) is

$$3{\cdot}5764x + 0{\cdot}1756y - 12{\cdot}226z = -5{\cdot}3907 \qquad (8)$$

and the deviations of the individual atoms from this plane are:

N(9) −0·0005, C(10) +0·0015, N(11) −0·0005 and N(12) −0·0005 Å.

The five hydrogen atoms, H(10) to H(14), of the guanidyl group, $-NHC(NH_2)_2^+$, are also very nearly in the plane of the NCNN, thus making the whole guanidyl group planar.

The average of the four C–C bond lengths in this molecule is 1·537 Å and the average of the four C–C–C angles is 111·0°. However, the angle C(4)–C(6)–C(7) at 114·4° is somewhat larger than the other three. A similar widening of the C–C–C angle adjacent to the amino group has been observed in other amino acids and peptides. The side chain including the guanidyl group is fully extended and lies approximately in a plane. The equation for the least-squares plane through these atoms is

$$3{\cdot}6684x - 0{\cdot}5873y - 11{\cdot}992z = -5{\cdot}6305 \qquad (9)$$

and the dihedral angle between this plane and the one through the acid group is 74°.

Packing of the molecules

The packing of the arginine molecules is characterized by a three-dimensional network of hydrogen bonds. A drawing of the structure viewed along the *a* axis is shown in Fig. 6. The arginine molecules lie extended parallel to the *c* axis and they form infinite chains by means of the hydrogen bonding between two of the NH of the guanidyl group and the two O of the carboxyl group. The guanidyl and carboxyl groups involved in the hydrogen bonding are approximately coplanar. The deviations of the carboxyl atoms from the least-squares plane through the guanidyl group (equation 8) are

O(1) −0·28, O(2) +0·06, and C(3) −0·05 Å.

Hydrogen bonding between arginine molecules also occurs parallel to the *b* axis in which O(2) from the carboxyl group is bonded to N(12′)H(14′) of the

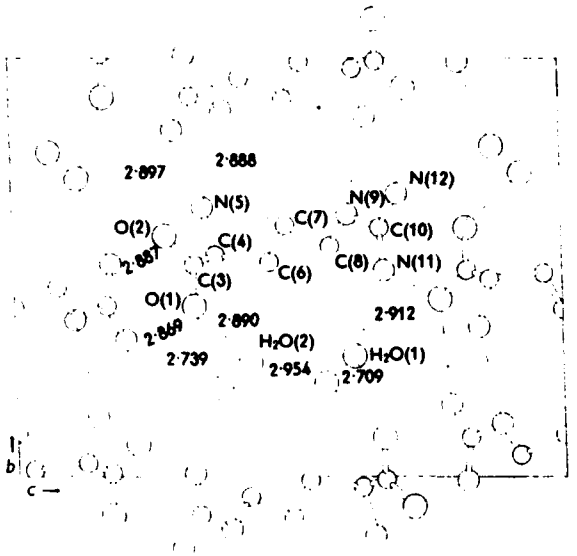

Fig. 6. A drawing of the structure of L-arginine dihydrate viewed along the *a* axis. The dashed lines indicate the hydrogen bonding.

guanidyl group and N(9′)H(10′) of the guanidyl group is bonded to N(5) of the amino group. The two hydrogen atoms, H(2) and H(3), in the amino group are not involved in hydrogen bond formation. This is a rather unusual occurrence. It is expected that molecules in a crystal usually arrange themselves to form a maximum number of hydrogen bonds (see, *e.g.*, Fuller, 1959).

The water molecules form infinite chains perpendicular to the arginine chains and parallel to the *a* axis by hydrogen bonding to each other. In addition, the water molecules form lateral hydrogen bonds to the arginine molecules. They are the donors of two hydrogen bonds and the acceptor for one.

The hydrogen bond lengths and angles are listed in Table 5. The values are consistent with those found in many other crystals (Fuller, 1959). The four hydrogen bonds around *W*(1), the oxygen atom in $H_2O(1)$, are arranged in a roughly tetrahedral configuration, whereas the three hydrogen bonds around *W*(2) are approximately in a plane.

The closest intermolecular approaches between non-bonded atoms are those between N(5) and N(12′) (3·42 Å), and between N(5) and N(11″) (3·36 Å), where hydrogen bonds may have been expected to form, and 3·45 Å between two water molecules not hydrogen-bonded to each other.

Table 5. *Hydrogen-bonds lengths and angles*

Bond		Angle	
N(9)H(10)···N(5′)	2·888 Å	C(8)N(9)···N(5′)	112·7°
		C(10)N(9)···N(5′)	110·5
N(12)H(14)···O(2′)	2·897	C(10)N(12)···O(2′)	135·6
N(12)H(13)···O(1″)	2·869	C(10)N(12)···O(1″)	116·3
N(11)H(12)···O(2″)	2·887	C(10)N(11)···O(2″)	121·2
W(1)H(15)···O(1′)	2·739	N(11)···*W*(1)···*W*(2)	101·7
N(11)H(11)···*W*(1)	2·912	N(11)···*W*(1)···O(1′)	109·9
W(2)H(18)···*W*(1)	2·954	N(11)···*W*(1)···*W*(2′)	138·0
W(1)H(16)···*W*(2′)	2·709	*W*(2)···*W*(1)···O(1′)	105·6
W(2)H(17)···O(1)	2·890	*W*(2)···*W*(1)···*W*(2′)	78·8
		W(2′)···*W*(1)···O(1′)	110·2
		O(1)···*W*(2)···*W*(1)	122·4
		O(1)···*W*(2)···*W*(1′)	120·0
		W(1)···*W*(2)···*W*(1′)	116·2

We wish to acknowledge the invaluable assistance of Mr. Peter Gum, who performed all the high-speed machine calculations and programmed many of the routines for the IBM 7090 and IBM 7030 (STRETCH).

References

Bryden, J. H., Burkardt, L. A., Hughes, E. W. & Donohue, J. (1956). *Acta Cryst.* **9**, 573.

Busing, W. R., Martin, K. O. & Levy, H. A. (1962). ORFLS, Oak Ridge National Laboratory, Oak Ridge, Tennessee, U.S.A.

Drenth, J., Drenth, W., Vos, A. & Wiebenga, E. H. (1953). *Acta Cryst.* **6**, 424.

Fuller, W. (1959). *J. Phys. Chem.* **63**, 1705.

Hauptman, H. & Karle, J. (1956). *Acta Cryst.* **9**, 45.

Karle, I. L., Britts, K. & Gum, P. (1964). *Acta Cryst.* **17**, 496.

Karle, I. L., Hauptman, H., Karle, J. & Wing, A. B. (1958). *Acta Cryst.* **11**, 257.

Karle, I. L. & Karle, J. (1963). *Acta Cryst.* **16**, 969.

Karle, J. & Hauptman, H. (1956). *Acta Cryst.* **9**, 635.

Karle, J. & Hauptman, H. (1958). *Acta Cryst.* **11**, 264.

Karle, J. & Hauptman, H. (1964). *Acta Cryst.* **17**, 392.

Marsh, R. E. (1958). *Acta Cryst.* **11**, 654.

Sklar, N., Senko, M. & Post, B. (1961). *Acta Cryst.* **14**, 716.

Wright, D. A. & Marsh, R. E. (1962). *Acta Cryst.* **15**, 54.

Proc. Natl. Acad. Sci. USA
Vol. 88, pp. 5307–5311, June 1991
Biochemistry

Crystal structure of [Leu^1]zervamicin, a membrane ion-channel peptide: Implications for gating mechanisms

(x-ray diffraction/channel mouth/helix bending/polymorphs/α-alkyl amino acids)

ISABELLA L. KARLE*, JUDITH L. FLIPPEN-ANDERSON*, SANJAY AGARWALLA†, AND PADMANABHAN BALARAM†

*Laboratory for the Structure of Matter, Naval Research Laboratory, Washington, DC 20375-5000; and †Molecular Biophysics Unit, Indian Institute of Science, Bangalore 560 012, India

Contributed by Isabella L. Karle, March 21, 1991

ABSTRACT **Structures in four different crystal forms of [Leu^1]zervamicin (zervamicin Z-L, Ac-Leu-Ile-Gln-Iva-Ile^5-Thr-Aib-Leu-Aib-Hyp^{10}-Gln-Aib-Hyp-Aib-Pro^{15}-Phol, where Iva is isovaline, Aib is α-amino isobutyric acid, Hyp is 4-hydroxyproline, and Phol is phenylalaninol), a membrane channel-forming polypeptide from *Emericellopsis salmosynnemata*, have been determined by x-ray diffraction. The helical structure is amphiphilic with all the polar moieties on the convex side of the bent helix. Helices are bent at Hyp^{10} from ≈30° to ≈45° in the different crystal forms. In all crystal forms, the peptide helices aggregate in a similar fashion to form water channels that are interrupted by hydrogen bonds between N^{e}H(Gln^{11}) and O$^\delta$(Hyp^{10}) of adjacent helices. The Gln^{11} side chain is folded in an unusual fashion in order to close the channel. Space is available for an extended conformation for Gln^{11}, in which case the channel would be open, suggesting a gating mechanism for cation transport. Structural details are presented for one crystal form derived from methanol/water solution: $C_{85}H_{140}N_{18}O_{22}\cdot 10H_2O$, space group $P2_1$, a = 23.068(6) Å, b = 9.162(3) Å, c = 26.727(9) Å, β = 108.69(2)° (standard deviation of last digit is given in parentheses); overall agreement factor R = 10.1% for 5322 observed reflections [$|F_o| > 3\sigma(F)$]; resolution, 0.93 Å.**

Several acyclic, α-aminoisobutyric acid (Aib)-containing polypeptides of fungal origin (Fig. 1) form voltage-gated channels in phospholipid bilayer membranes (1–6). The best studied members of this class are alamethicins, 20-residue peptides for which a crystal structure has been reported at 1.5-Å resolution (3). Several models for alamethicin ion channels have been proposed (3–6), based on the helical conformation observed in crystals. The molecular packing in alamethicin crystals, however, did not directly provide a model for a membrane-phase channel aggregate (3). The zervamicins are a related class of peptides isolated from cultures of *Emericellopsis salmosynnemata* (7). These peptides are shorter (16 residues) than alamethicin and contain several polar residues (Thr, Gln, Hyp) distributed evenly throughout the sequence (8). A preliminary report suggests that zervamicins exhibit lower pore-forming ability and enhanced antibacterial properties compared with alamethicin (8). More recently, the zervamicins have been shown to form voltage-dependent multilevel ion channels in bilayer membranes (ref. 9; M. S. P. Sansom, personal communication). Although the conductive activity is qualitatively similar to that of alamethicin, the kinetics of switching between states is appreciably faster for zervamicins. The major polypeptide components of zervamicin (IIA and IIB) contain a Trp residue at position 1. During HPLC fractionation, a minor component containing Leu at position 1, [Leu^1]zervamicin (zervamicin Z-L), has been isolated. The component has been crystallized and the structure determined in four different crystal forms to resolutions as high as 0.93 Å and R = 10.1% (Table 1). In each of the four different crystal forms, space groups $P2_1$ and $P2_12_12_1$, the peptide molecules associate to form similar discontinuous water channels, which appear to give further insights into the nature of an ion channel, a possible gating mechanism, and the dynamics of a bent helix molecule.

Alamethicin I (II)	Ac-Aib-Pro-Aib-Ala-Aib^5-Ala(Aib)-Gln-Aib-Val-Aib^{10}-Gly-Leu-Aib-Pro-Val^{15}-Aib-Aib-Glu-Gln-Phol^{20}
Antiamoebin I (II)	Ac-Phe-Aib-Aib-Aib-D-Iva^5-Gly-Leu-Aib-Aib-Hyp^{10}-Gln-D-Iva-Hyp(Pro)-Aib-Pro^{15}-Phol
Zervamicin IIA (IIB)	Ac-Trp-Ile-Gln-Aib(Iva)-Ile^5-Thr-Aib-Leu-Aib-Hyp^{10}-Gln-Aib-Hyp-Aib-Pro^{15}-Phol
Zervamicin Z-L	Ac-Leu-Ile-Gln-Iva-Ile^5-Thr-Aib-Leu-Aib-Hyp^{10}-Gln-Aib-Hyp-Aib-Pro^{15}-Phol

FIG. 1. Sequences of some Aib-containing antibiotics that transport ions across membranes. Phol, phenylalaninol; Iva, isovaline (α-ethylalanine); Hyp, 4-hydroxyproline.

EXPERIMENTAL PROCEDURES

[Leu^1]Zervamicin was isolated from a heterogeneous zervamicin mixture by HPLC on a reverse-phase C_{18} column, as described (10). Crystals were grown by slow evaporation of methanol/water solution or by vapor diffusion of water into ethylene glycol/ethanol solutions containing about 3 mg of peptide in 0.4 ml of solvent. X-ray diffraction data were measured with a four-circle automated diffractometer with CuK_α radiation on crystals under the conditions listed in Table 1 for a best set of data. Lowering the temperature for some of the crystal forms resulted in shattering the crystal. Rapid scan speeds, 7–15°/min, were used in order to collect most of the data before significant deterioration of the crystal. The structures were solved by a vector-search procedure (11) contained in the SHELX84 package of programs (MicroVAX version of the SHELXTL system of programs; Siemens Instruments, Madison, WI). The search model was based on the backbone atoms of the known structure of a 16-residue apolar analog of zervamicin (12) and was followed by a partial-structure procedure (13) by which the atoms in the side chains were located. The detailed structure only of crystal A will be reported here. Full-matrix anisotropic least-squares refine-

The publication costs of this article were defrayed in part by page charge payment. This article must therefore be hereby marked "*advertisement*" in accordance with 18 U.S.C. §1734 solely to indicate this fact.

Abbreviations: Aib, α-aminoisobutyric acid (α-methylalanine); Hyp, 4-hydroxyproline; Iva, isovaline (α-ethylalanine); Phol, phenylalaninol.

Table 1. Crystal parameters for Ac-Leu-Ile-Gln-Iva-Ile-Thr-Aib-Leu-Aib-Hyp-Gln-Aib-Hyp-Aib-Pro-Phol, $C_{85}H_{140}N_{18}O_{22}\cdot xH_2O$

Parameter	Crystal A*†	Crystal B†	Crystal C	Crystal D
Space group	$P2_1$	$P2_1$	$P2_12_12_1$	$P2_12_12_1$
Cell dimensions				
a, Å	23.068(6)	21.857(4)	10.337(2)	10.160(3)
b, Å	9.162(3)	9.381(3)	28.389(7)	28.252(9)
c, Å	26.727(9)	26.744(6)	39.864(11)	40.338(9)
β, degrees	108.69(2)	105.22(2)	90	90
Growth solvent	CH_3OH/H_2O	CH_3OH/H_2O	$HOCH_2CH_2OH$	‡
No. of reflections				
$[\|F_o\| > 3\sigma(F)]$	5322	2939	4239	2251
Crystal condition	−45°C, dry	20°C, dry	20°C, in capillary	20°C, in capillary
Volume per asymmetric unit, Å^3	2676	2638	2924	2895

*$R = \Sigma||F_o| - |F_c||/\Sigma|F_o|$ for all data with $|F_o| > 3\sigma(F)$ = 10.1%; resolution, 0.93 Å. Estimated SDs for backbone: ≈0.023 Å (bonds); ≈1.3° (angles). Estimated SDs for side chains: ≈0.03 Å (bonds); ≈1.7° (angles).

†Crystals A and B were present in the same crystallizing vial.

‡Crystal D was obtained by soaking crystal C in aqueous KCl (no K^+ in crystal D); approximate coordinates for the peptide are known, but least-squares refinement was not completed.

ment was performed on the C, N, and O atoms in the peptide, after which H atoms were placed in idealized positions with C–H distances of 0.96 Å and allowed to ride with the C or N atoms to which each was bonded for the final cycles of refinement. The thermal factors for the H atoms were fixed at U_{iso} = 0.125. Water molecules for a total of 11 sites (one pair of sites is mutually exclusive) were located in a series of difference maps and added stepwise to the refinement. The phenyl group in the Phol residue was constrained to be a regular hexagon with C–C distances of 1.395 Å, although the position and orientation of the hexagon and the isotropic thermal values for each atom in the hexagon were subjected to least-squares refinement. Finally, the amide moiety in the Gln[3] side chain, particularly the $N^{\epsilon}(3)$ atom (in all the crystal forms) was particularly mobile; therefore the bond lengths and bond angles in the $-C(O)NH_2$ moiety were constrained to reasonable values while the orientation of the amide group and the isotropic thermal factors associated with the $C^{\delta}(3)$, $O^{\epsilon}(3)$, and $N^{\epsilon}(3)$ atoms were allowed to vary in the least-squares process. With the above constraints, and not quite a full sphere of data to a resolution of 0.93 Å due to the onset of crystal deterioration, the final R factor is 10.1% for 5322 data observed with $|F_o| > 3\sigma(F)$. Bond lengths and bond angles (estimated SD, approximately 0.02 Å for bonds and 1.2° for angles) do not show significant or systematic differences from expected values.‡

RESULTS

The Peptide Helix. Both alamethicin and zervamicin have a high proportion of Aib residues, which are strong helix formers (14–16). Zervamicin has polar moieties in residues 3, 6, 10, 11, 13, and 16. As expected for a helical structure with polar residues spaced at each third or fourth position (17, 18), all of these polar moieties are on one side of the zervamicin helix (Fig. 2), thus giving the helix an amphiphilic character. Although Gln[11] would appear to break the rule, the torsions about the C^{α}—C^{β} and C^{β}—C^{δ} bonds in Gln[11] are −51° and −55°, respectively, which fold the polar $-C(O)NH_2$ group back from the nonpolar face to the polar face of the helix. The unusual conformation and the probable mobility of the Gln[11] side chain strongly suggest the location of the gating mechanism during ion transport (see below). Additionally, the polar face is enhanced by the exposed backbone carbonyl oxygens in residues 6, 7, and 10, which do not participate in intrahelical hydrogen bonds (Table 2) due to the presence of Hyp[10] and Hyp[13]. These carbonyls are available for hydrogen bonding to the neighboring water molecules or another peptide molecule or for making transient ligands with cations that are being transported.

Despite the presence of two Hyp residues and one Pro residue, the backbone is entirely helical. Torsional angles are listed in Table 3. An α-helix is formed from the amino terminus through the ninth residue. A β-ribbon containing Hyp[10], Hyp[13], and Pro[15] is twisted into a helix that extends to the carboxyl terminus. The helix is bent at Hyp[10], giving the peptide an overall banana shape. It is interesting that the

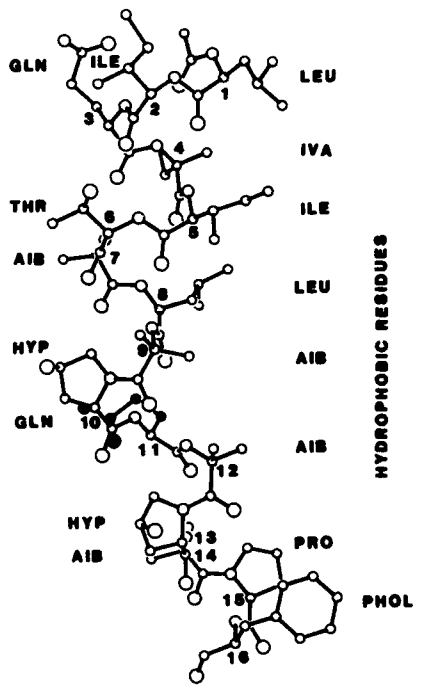

FIG. 2. Conformation of [Leu[1]]zervamicin drawn with the coordinates obtained from crystal A. The C^{α} atoms are labeled 1–16. The side chain in Gln[11] (filled circles) is not extended to the hydrophobic face but folded backward to the polar face of the helix.

‡Supplementary material consisting of atomic coordinates for C, N, and O atoms, bond lengths and angles, anisotropic thermal factors, and coordinates for hydrogen atoms has been deposited with the Cambridge Structural Data Base, University Chemical Laboratory, Lensfield Road, Cambridge CB2 IEW, U.K. Lists of observed and calculated structure factors are available from I.L.K. and J.L.F.-A.

Table 2. Hydrogen bonds

Peptide helix						Water structure		
Type	Donor	Acceptor	N···O or O···O, Å	H···O,* Å	C=O···N angle, degrees	Donor	Acceptor	N···O or O···O,* Å
Head-to-tail	N(1)	O(15)†	2.93	2.04	122	W(1)	$O^{\gamma}(6)$§	2.82
	N(2)	O(16)†	2.96	2.07	140	W(1)	O(10)	3.00
Intramolecular	N(3)	$O^{\varepsilon}(3)$	3.07	2.32		W(2)	O(3)‡	2.91
5 → 1	N(4)	O(0)	2.85	2.01	167	W(2)	W(1)	2.82
	N(5)	O(1)	3.15	2.26	158	W(3)	$O^{\delta}(13)$	3.21
	N(6)	O(2)	3.25	2.40	146	W(3)	W(2)	2.82
Intramolecular	$O^{\gamma}(6)$	O(2)	2.79	1.97		W(4A)	W(3)	2.50
5 → 1	N(7)	O(3)	2.88	2.03	155	W(4B)	W(3)	2.89
	N(8)	O(4)	3.36	2.60	131	$N^{\varepsilon}(3)$§	W(4B)	3.08
	N(9)	O(5)	2.98	2.26	165	W(5)	W(4A)	2.98
Intermolecular	$O^{\delta}(10)$‡	O(7)	2.75	1.91		W(5)	W(6)	3.08
	$N^{\varepsilon}(11)$§	O(6)	3.09	2.22		W(6)	O(14)	2.90
	$N^{\varepsilon}(11)$§	$O^{\delta}(10)$	2.91	2.06		W(6)†	$O^{\varepsilon}(3)$	2.73
β-Ribbon	N(11)	O(8)	2.88	2.01	138	O(16)	W(6)	2.67
	N(12)	O(9)	3.15	2.26	124	W(7)	W(5)	2.48
Intermolecular	$O^{\delta}(13)$	$O^{\varepsilon}(11)$¶	2.67	1.85		W(8)	O(11)	3.00
β-Ribbon	N(14)	O(11)	3.01	2.12	129	W(8)	W(9)†	2.67
	N(16)	O(13)	2.82	1.99	129	W(9)	O(12)‖	2.94
						W(9)	W(8)	3.13
						W(10)	O(15)	3.15

*The H atoms were placed in idealized positions with the N–H distance equal to 0.96 Å.
†Symmetry equivalents $1 + x, y, 1 + z$ to coordinates listed in supplementary material (see footnote at end of *Experimental Procedures*).
‡Symmetry equivalents $2 - x, -\frac{1}{2} + y, 1 - z$.
§Symmetry equivalents $2 - x, \frac{1}{2} + y\ 1 - z$.
¶Symmetry equivalents $x, 1 + y, z$.
‖Symmetry equivalents $x, -1 + y, z$.

conformation of the backbone of a completely apolar synthetic analog of [Trp[1]]zervamicin (12) is almost identical to that of the backbone in the natural [Leu[1]]zervamicin. The configuration of the Iva residue at position 4 is *R*, confirming an earlier stereochemical assignment (8).

Channel Formation. The peptide molecules in all four polymorphs have very similar helical conformations, intramolecular hydrogen bonds, head-to-tail hydrogen bonds, and interpeptide hydrogen bonds. The differences in conformation are manifested mainly by the bend of the helix, 36° for A, 30° for B, and 45° for C (structure D is not sufficiently well refined at this time for us to make a measurement). In all the crystals, the polar faces associate in a common antiparallel fashion. Fig. 3 illustrates this association with a superposition of the envelopes of the structures, showing the peptide molecules A, B, and C. In the middle, the molecules in each

Table 3. Torsion angles* (degrees)

Residue	ϕ	ψ	ω	χ^1	χ^2	χ^3	χ^4
Leu^1	−51†	−45	−173	175	73, −169		
Ile^2	−63	−45	−178	164, −68	168		
Gln^3	−69	−40	−172	−67	85	15, −139‡	
Iva^4	−57	−54	−177	57			
Ile^5	−74	−35	176	172, −66	180		
Thr^6	−59	−44	−176	−64, 179§			
Aib^7	−59	−37	−171				
Leu^8	−91	−24	−171	−74	−75, 165		
Aib^9	−55	−39	−179				
Hyp^{10}	−63	−16	−177	−24	36	−35	19¶
Gln^{11}	−89	−9	179	−51	−54	−44, 135‖	
Aib^{12}	−51	−37	−177				
Hyp^{13}	−77	−6	−168	−21	34	−33	20**
Aib^{14}	−53	−44	−178				
Pro^{15}	−80	−13	−170	−10	24	−29	22††
$Phol^{16}$	−115	+72‡‡		−69	−75, 101		

The torsion angles for rotation about the bonds of the peptide backbone (ϕ, ψ, and ω) and about bonds of the amino acid side chains (χ^n) are described in ref. 19.
*Estimated SDs, ≈1.5°.
†C′(O),N(1),C^{α}(1),C′(1).
‡C^{β}(3),C^{γ}(3),C^{δ}(3),O^{ε}(3), +15°; C^{β}(3),C^{γ}(3),C^{δ}(3),N^{ε}(3), −139°.
§N(6),C^{α}(6),C^{β}(6),O^{γ}(6), −64°; N(6),C^{α}(6),C^{β}(6), C^{γ}(6), 179°.
¶C^{δ}(10),N(10),C^{α}(10),C^{β}(10), 3°; C^{α}(10),C^{β}(10),C^{γ}(10),O^{δ}(10), −81°.
‖C^{β}(11),C^{γ}(11),C^{δ}(11),O^{ε}(11), −44°; C^{β}(11),C^{γ}(11),C^{δ}(11), N^{ε}(11), 135°.
**C^{δ}(13),N(13),C^{α}(13),C^{β}(13), 1°; C^{α}(13),C^{β}(13),C^{γ}(13),O^{δ}(13), −83°.
††C^{δ}(15),N(15),C^{α}(15),C^{β}(15), −8°.
‡‡N(16),C^{α}(16),C(16)(CH_2OH),O(16)(CH_2OH).

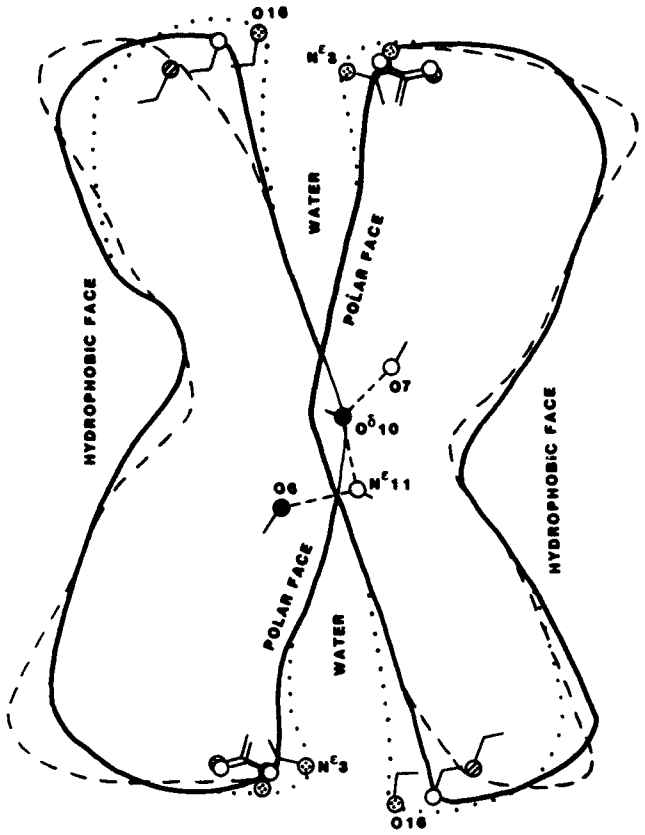

FIG. 3. Schematic diagram showing a superposition of the envelopes of [Leu[1]]zervamicin helices in crystal A (solid line), crystal B (dotted line), and crystal C (dashed line). The polar face of the helices associates in an antiparallel fashion and forms a discontinuous water channel that contains a different number of water molecules in each crystal form. The channel is closed in the middle by *inter*peptide hydrogen bonds involving backbone carbonyls O(6) and O(7) and side chain moieties $O^{\delta}(Hyp^{10})$ and $N^{\epsilon}(Gln^{11})$. The size of the mouth of the channel is determined by the movement of $O(Phol^{16})$ and $N^{\epsilon}(Gln^{3})$ in adjacent peptide molecules.

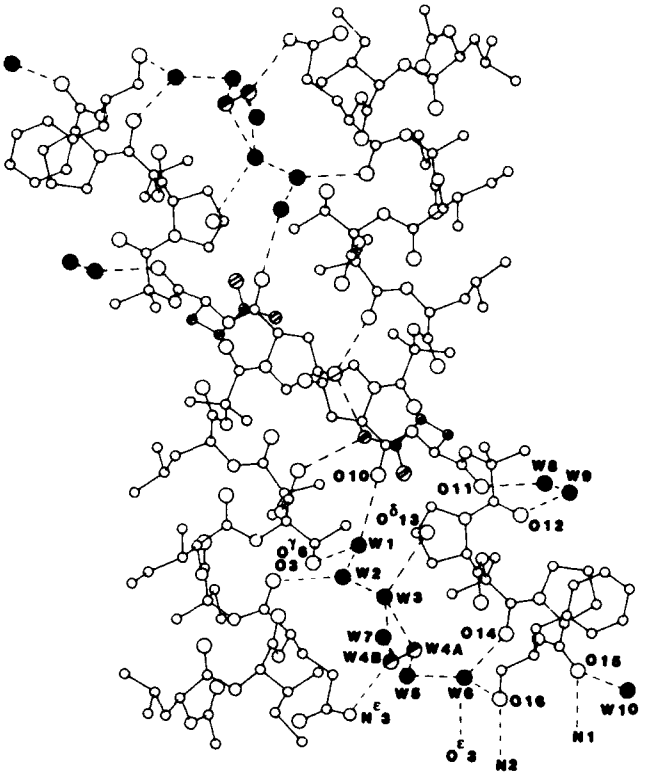

FIG. 4. Water molecules (●) in crystal A of [Leu[1]]zervamicin. The two peptide molecules are related by a twofold screw axis. The atoms in the side chain of Gln^{11} are marked with stripes. Hydrogen bonds are indicated by dashed lines.

crystal are held together with *inter*peptide hydrogen bonds $O(Thr^{6}) \cdots N^{\epsilon}(Gln^{11})$, $N^{\epsilon}(Gln^{11}) \cdots O^{\delta}(Hyp^{10})$, and $O^{\delta}(Hyp^{10}) \cdots O(Aib^{7})$. The banana-shaped molecules spread apart from each other at either end by differing amounts, related to the bend in each helix. The resulting cavities are filled with varying amounts of water depending upon the size of the cavity. For crystal A there are eight water sites (one disordered) at each end. These are shown in detail in Fig. 4, along with the hydrogen bonding between water molecules and between peptide and water molecules.

The mouth of the water cavity is constricted or expanded depending upon the bend in the helix. The $O(Phol^{16}) \cdots N^{\epsilon}(Gln^{3})$ separation is 3.7 Å in crystal B, 6.8 Å in crystal A, and >8 Å in crystal C. Despite the flexibility of the peptide, atom $O(Phol^{16})$ is relatively rigid since it participates in head-to-tail hydrogen bonding. The $-C(O)NH_2$ end of Gln^{3}, however, is quite mobile and $N^{\epsilon}(3)$ makes hydrogen bonds mainly to disordered or transient water sites. The carbonyl O(3) makes an *intra*helical hydrogen bond to the backbone N(3) moiety of the same residue in crystal A but not in crystal B.

Gating. A continuous water channel is not formed between the polar surfaces of adjacent peptide molecules. A view of the middle segments of adjacent molecules, where *inter*peptide hydrogen bonding takes place and closes the channel, is shown in Fig. 5. The view is perpendicular to that in Figs. 3 and 4 and is directed into the helices. Three molecules appear to define the closed channel. The side chain of Gln^{11} is not extended as Gln^{7} of alamethicin (3) but is folded backward to form a hydrogen bond with $O^{\delta}(Hyp^{10})$. The Hyp residue is quite rigid. It is conceivable that under the application of a potential, the Gln^{11} side chain can open the channel by

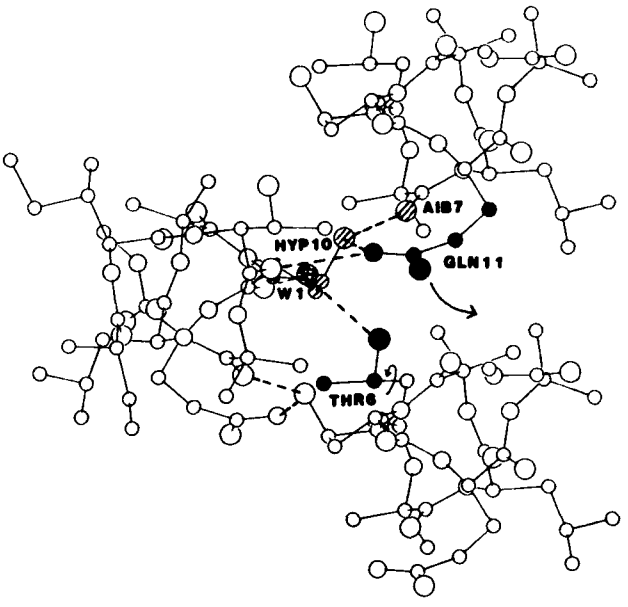

FIG. 5. A possible gating mechanism by Gln^{11} and Thr^{6} in channels formed by [Leu[1]]zervamicin. The view of the closed channel is perpendicular to the orientation in Figs. 3 and 4. Only the middle residues of three adjacent peptide molecules are shown. The water molecule closest to the closed portion of the channel is W(1) (checkered). The carbonyl oxygen in Aib^{7} and the hydroxyl in Hyp^{10} (striped) are relatively rigid moieties and may define a boundary of a hypothetical open channel.

rotating into the adjacent space at the right (Fig. 5). If a column of water is pushed through the channel in a single file by a cation (20), it may also be possible that the side chain in Thr^6 can rotate about the C^α—C^β bond to further enlarge the channel. As shown in Fig. 4, there are many carbonyl, hydroxyl, and amino moieties along the channel to provide ligands for a cation that is being transported.

Nonpolar Face of Helix. Helical peptides forming a channel across a membrane would have their nonpolar side facing the membrane. The molecular recognition and aggregation of apolar helical peptides are not particularly selective. Such helical peptides have been found to crystallize with the helix axes either in an all-parallel motif or in an antiparallel motif. Even peptides with the same sequence have either all-parallel or antiparallel aggregation in different crystal forms (21, 22). Similarly in [Leu^1]zervamicin, in crystals A and B (space group $P2_1$), the nonpolar face of the helix associates in an antiparallel fashion, while in crystals C and D (space group $P2_12_12_1$), the nonpolar face associates in a parallel fashion. The inference can be drawn that the nonpolar face is also fairly insensitive to the helix axis direction with respect to the membrane.

DISCUSSION

[Leu^1]zervamicin is a bent helical molecule, 29 Å long, with all the polar side chains on the convex side and the nonpolar side chains on the concave side. Alamethicin (3), also a bent helix, has a much smaller degree of bending and has fewer polar moieties on the convex face (Fig. 1). The helix in both peptides is flexible as shown by different amounts of bending in the three conformers in the same crystal of alamethicin and the four conformers in four different polymorphs of [Leu^1]-zervamicin. Although complex irregular water channels were observed in the alamethicin crystals, the polar residues are not directed toward the center of the channel as might be expected for a membrane ion channel (3). In each of the four crystal forms of [Leu^1]zervamicin, the polar faces of adjacent peptide molecules form the boundary of a water channel.

The molecular recognition of the nonpolar side of [Leu^1]zervamicin is not very specific. Either parallel or antiparallel association takes place in the different crystal forms. In contrast, the polar face is very specific in forming an antiparallel association with an adjacent molecule and a hydrogen bond between Hyp^{10} and Gln^{11}, among others. The $Hyp^{10} \cdots Gln^{11}$ hydrogen bond interrupts the water channel. The remarkable observation is that the Gln^{11} side chain has to reverse its direction, in a swinging-arm fashion, to approach the Hyp^{10} of an adjacent, antiparallel peptide. It may be indicative of the gating mechanism in ion transport under the application of a potential. The size of the water channel near its interruption is restricted to one water molecule or one cation. The implications from the crystal structure analyses are that the water channel is not an open channel—i.e., that there is no passive diffusion of cations. This point has been emphasized further by soaking crystals in KCl solution for various times at various concentrations. Short of the crystal cracking and disintegrating, the soaking produced crystals with somewhat different cell parameters, but with no K^+ penetration.

Time-resolved fluorescence anisotropy measurements on helical bilayer-spanning 21-residue peptides have shown that the amplitude of fast fluctuations are largest at the helix ends and decrease toward the center of the helix (23). The four crystal structures show an expansion or constriction of the mouth of the channel, $O(16) \cdots Gln^3$, that varies from 3.7 Å to >8.0 Å. The cation may be trapped in the channel by constriction of the mouth (24).

One of the interesting implications of the crystal structure of [Leu^1]zervamicin is the role played by the mobility of the long side chain of Gln residues: the demonstrated mobility of Gln^3 in controlling the size of the mouth of the water channel, and the implied mobility of Gln^{11} (by its unusual conformation) in probable participation in the gating mechanism. For proteins, the role of Gln residues has been characterized as relatively indifferent and has no extreme properties or violent preferences (25). Perhaps one of the distinctive functions of this residue is in the regulation of ion-transport peptides.

This research was supported in part by National Institutes of Health Grant GM30902, in part by the Office of Naval Research, and in part by a grant from the Department of Science and Technology, India. S.A. was supported by a fellowship of the Council of Scientific and Industrial Research, India.

1. Mueller, P. & Rudin, D. O. (1968) *Nature (London)* **217**, 713–719.
2. Nagaraj, R. & Balaram, P. (1981) *Acc. Chem. Res.* **14**, 356–362.
3. Fox, R. O. & Richards, F. M. (1982) *Nature (London)* **300**, 325–330.
4. Mathew, M. K. & Balaram, P. (1983) *Mol. Cell Biochem.* **50**, 47–64.
5. Hall, J. E., Vodyanoy, I., Balasubramanian, T. M. & Marshall, G. R. (1984) *Biophys. J.* **45**, 233–247.
6. Menestrina, G., Voges, K.-P., Jung, G. & Boheim, G. (1986) *J. Membr. Biol.* **93**, 111–132.
7. Argoudelis, A. D. & Johnson, L. E. (1974) *J. Antibiot.* **27**, 274–282.
8. Rinehart, K. L., Jr., Gaudioso, L. A., Moore, M. L., Pandey, R. C., Cook, J. C., Jr., Barber, M., Sedgwick, R. D., Bordoli, R. S., Tyler, A. N. & Green, B. N. (1981) *J. Am. Chem. Soc.* **103**, 6517–6520.
9. Mellor, I. R., Sansom, M. S. P., Krishna, K. & Balaram, P. (1989) in *Ion Transport*, eds. Keeling, D. & Benham, C. (Academic, New York), pp. 316–318.
10. Krishna, K., Sukumar, M. & Balaram, P. (1990) *Pure Appl. Chem.* **62**, 1417–1420.
11. Egert, E. & Sheldrick, G. M. (1985) *Acta Crystallogr. Sect. A* **41**, 262–268.
12. Karle, I. L., Flippen-Anderson, J., Sukumar, M. & Balaram, P. (1987) *Proc. Natl. Acad. Sci. USA* **84**, 5087–5091.
13. Karle, J. (1968) *Acta Crystallogr. Sect. B* **24**, 182–186.
14. Toniolo, C., Bonora, G. M., Bavoso, A., Benedetti, E., di Blasio, B., Pavone, V. & Pedone, C. (1983) *Biopolymers* **22**, 205–215.
15. Marshall, G. R., Hodgkin, E. E., Langs, D. A., Smith, G. D., Zabrocki, J. & Leplawy, M. T. (1990) *Proc. Natl. Acad. Sci. USA* **87**, 487–491.
16. Karle, I. L. & Balaram, P. (1990) *Biochemistry* **29**, 6747–6756.
17. Schiffer, M. & Edmundson, A. B. (1967) *Biophys. J.* **7**, 121–135.
18. Kaiser, E. T. & Kezdy, F. J. (1984) *Science* **223**, 249–255.
19. IUPAC-IUB Commission on Biochemical Nomenclature (1970) *Biochemistry* **9**, 3471–3479.
20. Stankovic, C. J., Heinemann, S. H. & Schreiber, S. L. (1990) *J. Am. Chem. Soc.* **112**, 3702–3704.
21. Karle, I. L., Flippen-Anderson, J. L., Sukumar, M. & Balaram, P. (1990) *Int. J. Pept. Protein Res.* **35**, 518–526.
22. Karle, I. L., Flippen-Anderson, J. L., Uma, K. & Balaram, P. (1990) *Biopolymers* **29**, 1835–1845.
23. Vogel, H., Nilsson, L., Rigler, R., Voges, K.-P. & Jung, G. (1988) *Proc. Natl. Acad. Sci. USA* **85**, 5067–5071.
24. Miller, C. (1989) *Neuron* **2**, 1195–1205.
25. Richardson, J. S. & Richardson, D. C. (1990) in *Prediction of Protein Structure and the Principles of Protein Conformation*, ed. Fasman, G. D. (Plenum, New York), pp. 1–98.

Looking Back

What is Matter? Never Mind.
What is Mind? No Matter
Punch XXIX, 1855

Dr. Isabella Karle, today, working on a crystal structure analyses project in her laboratory at NRL. Dr. Isabella Karle came to NRL in 1946 from the University of Michigan with her husband Dr. Jerome Karle; where she was teaching freshman chemistry to engineering students.

Dr. Karle in 1964, the year she received the Navy Superior Civilian Service Award for outstanding achievements in molecular spectroscopy.

Dr. Isabella Karle about 1948 at the electron diffraction apparatus. Soon after coming to NRL, Jerome Karle designed the large and complicated apparatus which Isabella assembled, aligned and fine-tuned and used for experimentation that determined three-dimensional structure and vibrational motion in gaseous molecules.

Dr. Karle aligning a crystal on an X-ray camera in the late 1960s.

In 1980, RADM Baciocco, Chief of Naval Research, presented Dr. Karle the Robert Dexter Conrad Award, the highest honor for scientific achievement in the Navy.

Dr. Fred Saalfeld, Director of the Office of Naval Research, presenting the Secretary of the Navy Distinguished Achievement in Science Award in 1987 to Dr. Karle.

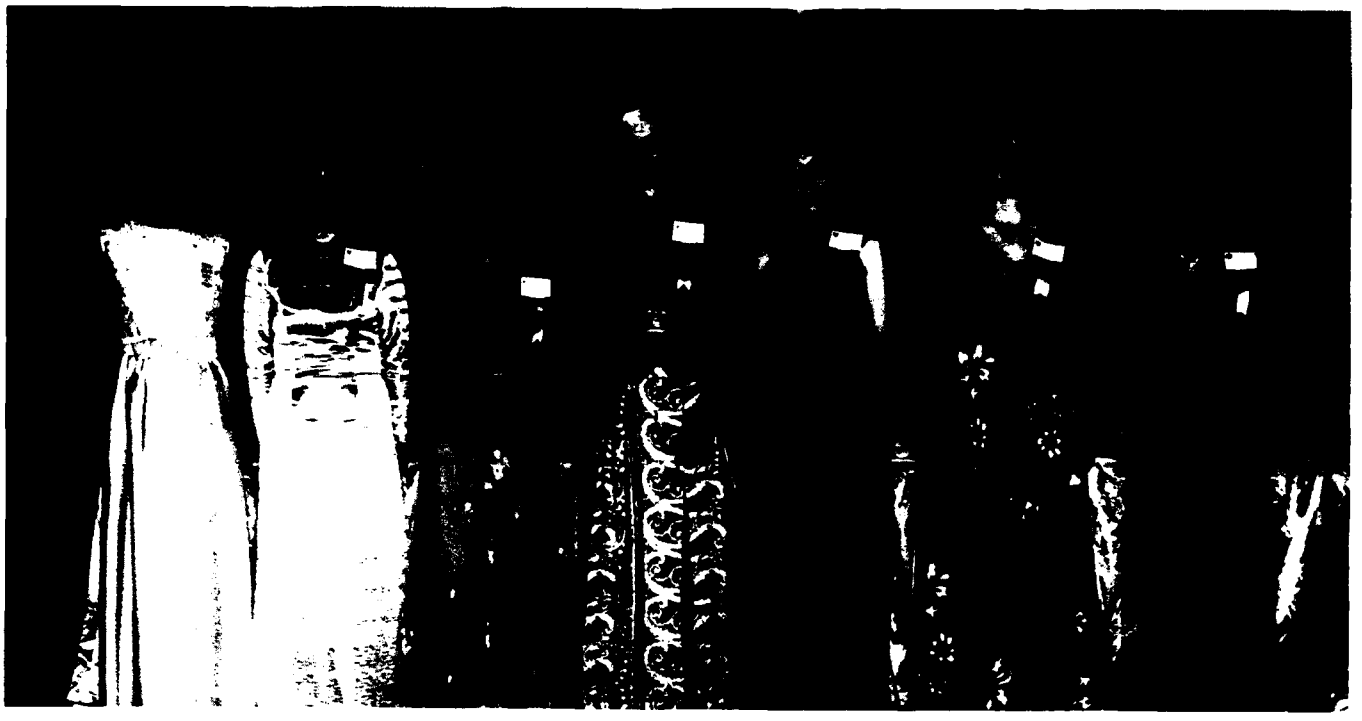

Dr Karle (second from right) on the occasion of receiving the Federal Women's Award in 1973.

Dr. Karle (right) when she received the degree of Doctor of Humane Letters, Georgetown University, in 1984.

Dr. Isabella and Dr. Jerome Karle have collaborated on many projects during their 47 years at NRL. It was Dr Isabella Karle who bridged the gap between the theory and experiment by translating mathematical results into practical procedures for determining the three dimensional structure of molecules.

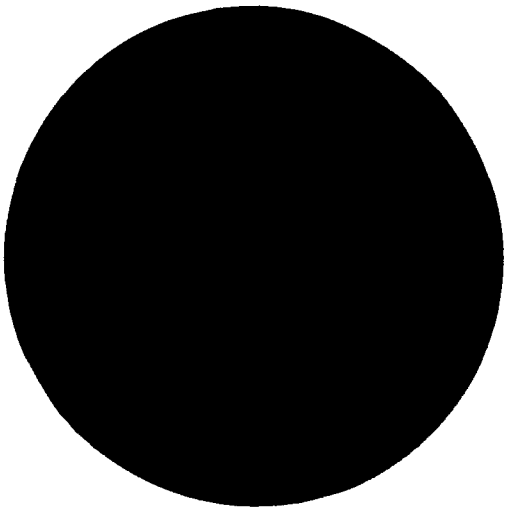

The Bower Award of The Franklin Institute

The Franklin Institute Of Philadelphia was founded in 1824 to promote scientific inquiry and to recognize scientific achievement. The Institute's Committee on Science and the Arts was founded in 1834 and serves as the Institute's science selection committee.

Through the careful work of this committee of scientists and engineers, the Franklin Institute was among the first to recognize the outstanding contributions of such individuals as Marie Curie and Albert Einstein. The Bower Award and Prize in Science was made possible by a $7.5 million bequest to the Franklin Institute by Henry Bower (1896-1988), a Philadelphia chemical manufacturer. The award, which consists of a gold medal and $250,000, is presented annually to a distinguished scientist of the world for outstanding work in the life or physical sciences. There is a rigorous process of nomination and review, involving national and international boards of advisors. The selection mission for this world-wide award is to find a person who reflects the scientific and humanitarian genius of Benjamin Franklin.

Aside from the Bower Award for Science, the Franklin Institute gives annually a Bower Award for Business, and 16 different medal awards.